

1 **Rare disease research workflow using multilayer networks elucidates the molecular**
2 **determinants of severity in Congenital Myasthenic Syndromes**

3 Iker Núñez-Carpintero ^{1,*}, Emily O'Connor ^{2,4,*}, Maria Rigau ^{1,5,6}, Mattia Bosio ^{1,7}, Yoshiteru
4 Azuma ^{8,9}, Ana Topf ^{10,11}, Rachel Thompson ², Peter A.C. 't Hoen ¹², Teodora Chamova ¹³,
5 Ivailo Tournev ^{13,14}, Velina Guerguelcheva ¹⁵, Steven Laurie ¹⁶, Sergi Beltran ^{16,17,18}, Salvador
6 Capella ^{1,7}, Davide Cirillo ^{1,#}, Hanns Lochmüller ^{2,3,4,16,19}, Alfonso Valencia ^{1,20}

7 ¹ *Barcelona Supercomputing Center (BSC), C/ Jordi Girona 29, 08034, Barcelona, Spain*

8 ² *Children's Hospital of Eastern Ontario Research Institute; Ottawa, Canada*

9 ³ *Division of Neurology, Department of Medicine, The Ottawa Hospital; Ottawa, Canada*

10 ⁴ *Brain and Mind Research Institute, University of Ottawa, Ottawa, Canada*

11 ⁵ *MRC London Institute of Medical Sciences, Du Cane Road, London, W12 0NN, United*
12 *Kingdom*

13 ⁶ *Institute of Clinical Sciences, Faculty of Medicine, Imperial College London, Hammersmith*
14 *Hospital Campus, Du Cane Road, London, W12 0NN, United Kingdom*

15 ⁷ *Spanish National Bioinformatics Institute Unit, Structural Biology and BioComputing*
16 *Programme, Spanish National Cancer Research Centre (CNIO), Madrid 28029, Spain*

17 ⁸ *Department of Human Genetics, Yokohama City University Graduate School of Medicine,*
18 *Yokohama, Japan*

19 ⁹ *Department of Pediatrics, Aichi Medical University, Nagakute, Japan*

20 ¹⁰ *John Walton Muscular Dystrophy Research Centre, Translational and Clinical Research*
21 *Institute, Newcastle University, Newcastle upon Tyne, United Kingdom*

22 ¹¹ *Newcastle Hospitals NHS Foundation Trust, Newcastle upon Tyne, United Kingdom*

23 ¹² *Center for Molecular and Biomolecular Informatics, Radboud Institute for Molecular Life*
24 *Sciences, Radboud university medical center, Nijmegen, The Netherlands*

25 ¹³ *Department of Neurology, Expert Centre for Hereditary Neurologic and Metabolic*
26 *Disorders, Alexandrovska University Hospital, Medical University-Sofia, Sofia, Bulgaria*

27 ¹⁴ *Department of Cognitive Science and Psychology, New Bulgarian University, Sofia 1618,*
28 *Bulgaria*

29 ¹⁵ *Clinic of Neurology, University Hospital Sofiamed, Sofia University St. Kliment Ohridski,*
30 *Sofia, Bulgaria.*

31 ¹⁶ *Centro Nacional de Análisis Genómico (CNAG-CRG), Center for Genomic Regulation,*
32 *Barcelona Institute of Science and Technology (BIST), Barcelona, Catalonia, Spain*

33 ¹⁷ *Universitat Pompeu Fabra (UPF), Barcelona, Spain*

34 ¹⁸ *Departament de Genètica, Microbiologia i Estadística, Facultat de Biologia, Universitat*
35 *de Barcelona (UB), Barcelona, Spain.*

36 ¹⁹ *Department of Neuropediatrics and Muscle Disorders, Medical Center – University of*
37 *Freiburg, Faculty of Medicine, Freiburg, Germany*

38 ²⁰ *ICREA, Pg. Lluís Companys 23, 08010, Barcelona, Spain*

39 * these authors contributed equally

40 # corresponding author: davide.cirillo@bsc.es

41 **Abstract**

42 Exploring the molecular basis of disease severity in rare disease scenarios is a challenging
43 task provided the limitations on data availability. Causative genes have been described for
44 Congenital Myasthenic Syndromes (CMS), a group of diverse minority neuromuscular
45 junction (NMJ) disorders; yet a molecular explanation for the phenotypic severity differences
46 remains unclear. Here, we present a workflow to explore the functional relationships between
47 CMS causal genes and altered genes from each patient, based on multilayer network analysis
48 of protein-protein interactions, pathways and metabolomics.

49 Our results show that CMS severity can be ascribed to the personalized impairment of
50 extracellular matrix components and postsynaptic modulators of acetylcholine receptor
51 (AChR) clustering. Moreover, reducing expression of the zebrafish orthologue, we confirm
52 the effect on movement and NMJ morphology of a gene previously unknown to be a NMJ
53 interactor, USH2A.

54 This work showcase how coupling multilayer network analysis with personalized -omics
55 information provides molecular explanations to the varying severity of rare diseases; paving
56 the way for sorting out similar cases in other rare diseases.

57 *Keywords:* multi-omics data, network biology, multilayer networks, personalized medicine,
58 applied network science, network community analysis, rare diseases, congenital myasthenic
59 syndromes.

60 Introduction

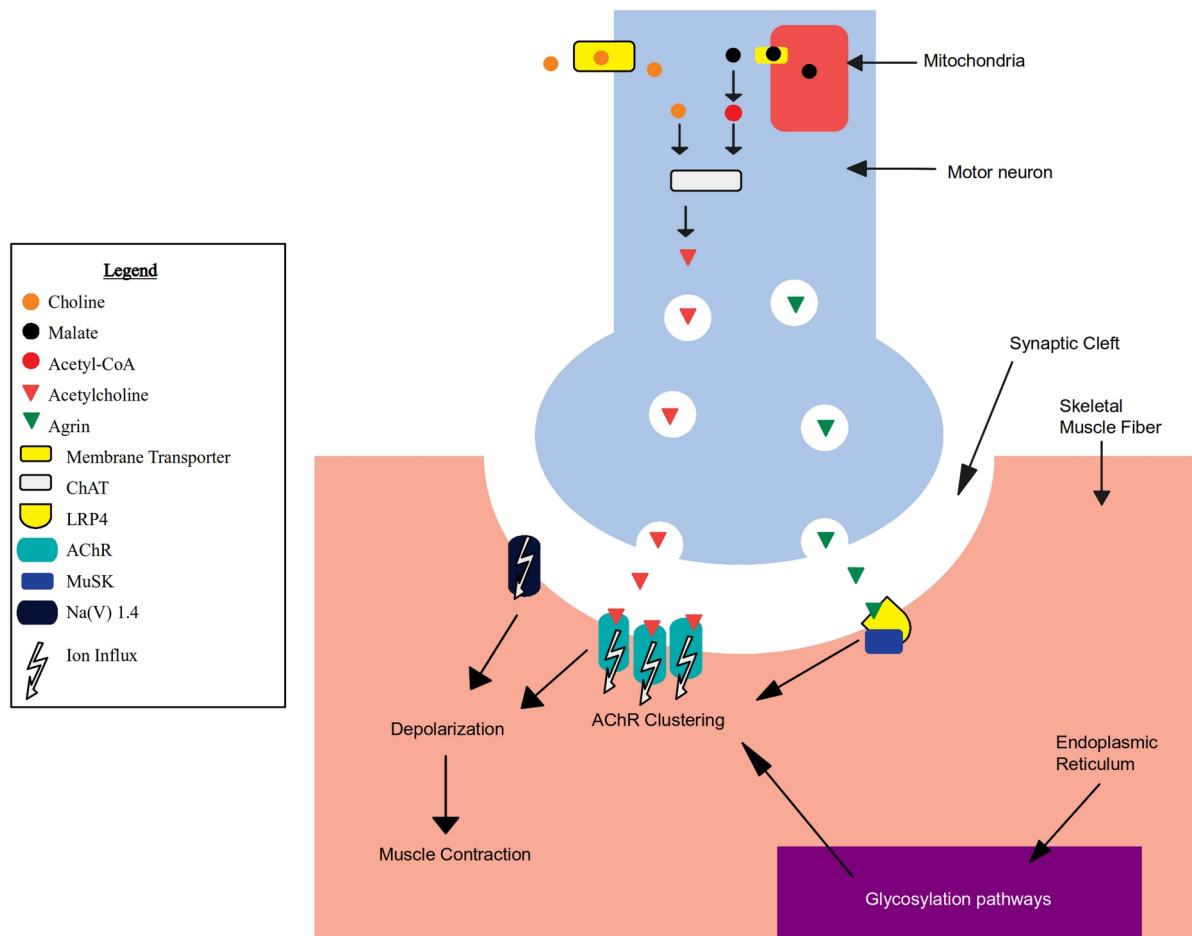
61 Understanding phenotypic severity is crucial for prediction of disease outcomes, as well as
62 for administration of personalized treatments. Different severity levels among patients
63 presenting the same medical condition could be explained by characteristic relationships
64 between diverse molecular entities (i.e. gene products, metabolites, etc) in each individual. In
65 this setting, multi-omics data integration is becoming a promising tool for research, as it has
66 the potential to gain complex insights of the molecular determinants underlying disease
67 heterogeneity. However, even in a scenario where the level of biomedical detail available to
68 study is growing in an exponential manner (Karczewski and Snyder, 2018), the analysis of
69 the molecular determinants of disease severity is not typically addressed in rare disease
70 research literature (Boycott et al. 2013), despite its obvious relevance at the medical and
71 clinical level. Rare diseases represent a challenging setting for the application of precision
72 medicine because, by definition, they affect a small number of patients, and therefore the data
73 available for study is considerably limited in comparison to other conditions. Accordingly,
74 leveraging the wealth of biomedical knowledge of diverse nature coming from publicly
75 available databases have the potential to address data limitations in rare diseases (Mitani and
76 Haneuse, 2020) (Buphamalai et al, 2021). In this sense, multilayer networks can offer an
77 holistic representation of biomedical data resources (Halu et al. 2017) (Gosak et al. 2018),
78 which may allow to explore the biology related to a given disease independently of cohort
79 sizes and their available omics data.

80 Here, in order to evaluate and demonstrate the potential of multilayer networks as means of
81 assessing severity in rare disease scenarios, we provide an illustrative case where we develop a
82 framework for analyzing a patient cohort affected by Congenital Myasthenic Syndromes
83 (CMS), a group of inherited rare disorders of the neuromuscular junction (NMJ). Fatigable
84 weakness is a common hallmark of these syndromes, that affects approximately 1 patient in
85 150,000 people worldwide. The inheritance of CMS is autosomal recessive in the majority of
86 patients. CMS can be considered a relevant use case because, while patients share similar
87 clinical and genetic features (Finsterer 2019), phenotypic severity of CMS varies greatly,
88 with patients experiencing a range of muscle weakness and movement impairment. While
89 over 30 genes are known to be monogenic causes of different forms of CMS (**Table 1**), these
90 genes do not fully explain the ample range of observed severities, which has been suggested
91 to be determined by additional factors involved in neuromuscular function (Thompson et al.
92 2019). Examples of CMS-related genes are AGRN, LRP4 and MUSK which code for
93 proteins that mediate communication between the nerve ending and the muscle, which is
94 crucial for formation and maintenance of the NMJ (**Figure 1**).

95 In particular, the AGRN-LRP4 receptor complex activates MUSK by phosphorylation,
96 inducing clustering of the acetylcholine receptor (AChR) in the postsynaptic membrane
97 allowing the presynaptic release of acetylcholine (ACh) to trigger muscle contraction
98 (Whicher, Philbin, and Aronson 2018). Additional evidence of CMS severity heterogeneity
99 emerged within the NeurOmics and RD-Connect projects (Lochmüller et al. 2018) studying a
100 small population (about 100 individuals) of gypsy ethnic origin from Bulgaria.

Location	Phenotype	Inheritance	Gene
2q31.1	CMS1A, slow-channel	AD	CHRNA1
2q31.1	CMS1B, fast-channel	AR, AD	
17p13.1	CMS2A, slow-channel	AD	CHRNB1
17p13.1	CMS2C, associated with acetylcholine receptor deficiency	AR	
2q37.1	CMS3 A, slow-channel	AD	CHRND
2q37.1	CMS3 B, fast-channel	AR	
2q37.1	CMS3 C, associated with acetylcholine receptor deficiency	AR	
17p13.2	CMS4 A, slow-channel	AR, AD	CHRNE
17p13.2	CMS4 B, fast-channel	AR	
17p13.2	CMS4 C, associated with acetylcholine receptor deficiency	AR	
3p25.1	CMS5	AR	COLQ
10q11.23	CMS6, presynaptic	AR	CHAT
1q32.1	CMS7, presynaptic	AD	SYT2
1p36.33	CMS8, with pre- and postsynaptic defects	AR	AGRN
9q31.3	CMS9, associated with acetylcholine receptor deficiency	AR	MUSK
4p16.3	CMS10	AR	DOK7
11p11.2	CMS11, associated with acetylcholine receptor deficiency	AR	RAPSN
2p13.3	CMS12, with tubular aggregates	AR	GFPT1
11q23.3	CMS13, with tubular aggregates	AR	DPAGT1
9q22.33	CMS14, with tubular aggregates	AR	ALG2
1p21.3	CMS15, without tubular aggregates	AR	ALG14
17q23.3	CMS16	AR	SCN4A
11p11.2	CMS17	AR	LRP4
20p12.2	CMS18	AD	SNAP25
10q22.1	CMS19	AR	COL13A1
2q12.3	CMS20, presynaptic	AR	SLC5A7
10q11.23	CMS21, presynaptic	AR	SLC18A3
2p21	CMS22	AR	PREPL
22q11.21	CMS23, presynaptic	AR	SLC25A1
15q23	CMS24, presynaptic	AR	MYO9A
12p13.31	CMS25, presynaptic	AR	VAMP1
3p21.31	CMS, related to GMPPB	AR	GMPBB
20q13.33	CMS, presynaptic	AR	LAMA5
3p21.31	CMS, with nephrotic syndrome	AR	LAMB2
8q24.3	CMS, with plectin defect	AR	PLEC
12q24.13	CMS, related to RPH3A	AR	RPH3A
9p13.3	CMS, presynaptic, related to MUNC13-1	AR	UNC13B
2q37.1	Escobar syndrome	AR	CHRNA1

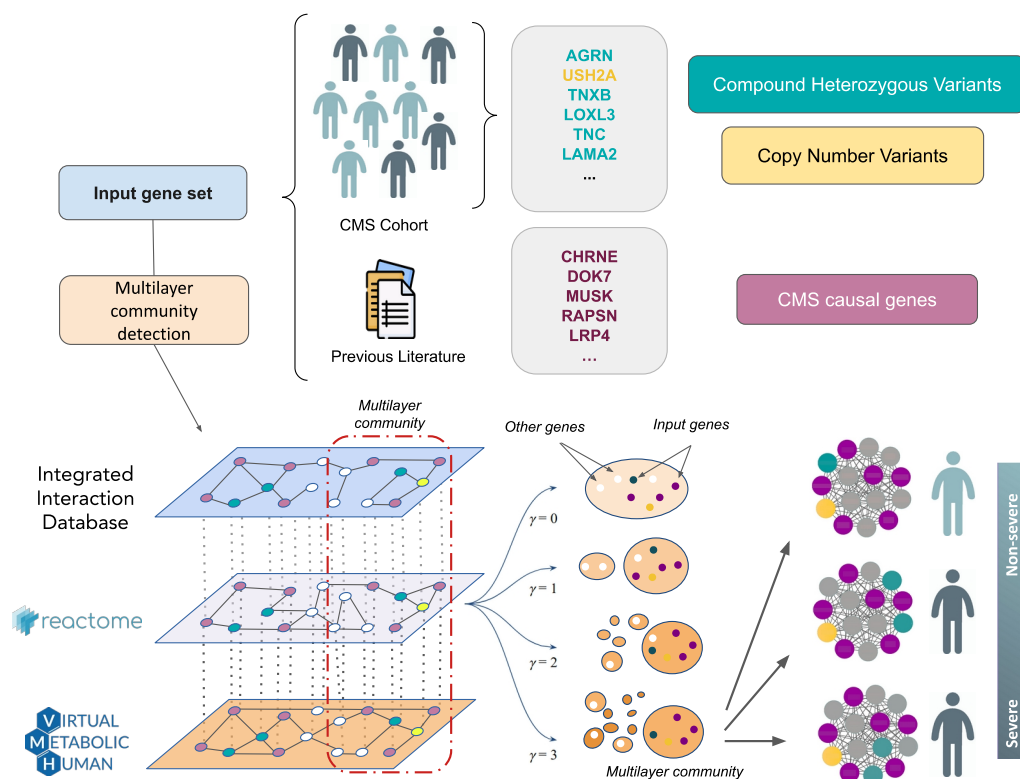
101 **Table 1.** Location, phenotype, inheritance and genes involved in CMS (adapted from
 102 <https://omim.org/phenotypicSeries/PS601462> and <http://www.musclegenetable.fr>). AR: autosomal
 103 recessive; AD: autosomal dominant.



104 **Figure 1.** A schematic depiction of the main molecular activities of known CMS causal genes
105 (Methods) taking place at the neuromuscular junction (NMJ) in the presynaptic terminal (in blue),
106 synaptic cleft (in white), and skeletal muscle fiber (in yellow) (for a detailed description of this system
107 see **Supplementary Information**).

108 All affected individuals shared the same causal homozygous mutation (a deletion within the
109 AChR ϵ subunit, *CHRNE* c.1327delG (A. Abicht et al. 1999)), however, the severity of
110 symptoms across this cohort varies considerably regardless of age, gender and initiated
111 therapy, suggesting the existence of additional genetic causes for the diversity of disease
112 phenotypes. By analyzing multi-omics data, we performed an in-depth characterization of 20
113 CMS patients, representing the two opposite ends of the spectrum observed in the wider
114 cohort, aiming to investigate the molecular basis of the observed differences in the individual
115 severity of the disease. Two CMS severity levels have been identified through extensive
116 phenotyping, namely a severe disease phenotype (8 patients) and a not-severe disease
117 phenotype (2 intermediate and 10 mild patients) (**Suppl. Table 1**). No demographic factor
118 (age, sex) nor clinical tests (speech, mobility, respiratory dysfunctions, among others) show a
119 significant association with the severity classes, with exception of Forced Vital Capacity
120 (FVC) and shoulder lifting ability (two-tailed Fisher's exact test p-values of 0.0128 and
121 0.0418, respectively; **Suppl. Figure 1**). We sought to interrogate whether severity was

119 determined by additional genetic variations impacting neuromuscular activity, on top of the
120 causative CHRNE mutation. We analyzed three main types of genetic variations: single
121 nucleotide polymorphisms (SNPs), copy number variations (CNVs), and compound
122 heterozygous variants (two recessive alleles located at different loci within the same gene in a
123 given individual). The extensive analysis of the genomic information did not render any
124 SNPs that could be considered a unique cause of disease severity by being common to all the
125 cases. Nevertheless, a number of CNVs and compound heterozygous variants were found to
126 appear exclusively in the different severity groups, in one or more patients. Moreover, the
127 compound heterozygous variants of the severe group are enriched in pathways related to the
128 extracellular matrix (ECM) receptors, which have been proposed as a target for CMS therapy
129 (Ito and Ohno 2018). To investigate the functional relationship between these variants and
130 CMS severity, **we designed an analytical workflow based on multilayer networks (Figure**
131 **2)**, allowing the integration of external biological knowledge to acquire deeper functional
132 insights. A multilayer network consists of several layers of nodes and edges describing
133 different aspects of a system (Kivelä et al. 2014). In biomedicine, this data representation has
134 been used to study biomolecular interactions (Zitnik and Leskovec 2017) and diseases (Halu
135 et al. 2017), facilitating integration and interpretation of heterogeneous sources of data.



136 **Figure 2.** Analytical workflow employed to address the severity of a cohort of patients affected by
137 Congenital Myasthenic Syndromes (CMS). A multi-scale functional analysis approach, based on
138 multilayer networks, was used to identify the functional relationships between genetic alterations
139 obtained from omics data (Whole Genome Sequencing, WGS; RNA-sequencing, RNAseq) with
140 known CMS causal genes. Modules of CMS linked genes are detected using graph community
141 detection at a resolution range (γ) (Methods) where the most prominent changes in community
142 structure occur. Modules that emerged from this analysis were characterized at single individual level.

143 Several established tools for network analysis have been recently adapted for multilayer
144 networks, such as random walk with restart (Valdeolivas et al. 2019), community detection
145 algorithms (Didier, Brun, and Baudot 2015) and node embeddings (Pio-Lopez et al. 2021).
146 By crossing patient genomic data with the information provided by a biomedical knowledge
147 multilayer network, we are able to describe the functional relationships of new genetic
148 modifiers responsible for the different phenotypic severity levels, showcasing the potential of
149 multilayer networks to provide support on the personalized analysis of rare disease patients.

150 **Results**

151 ***Variants do not segregate with patient severity***

152 We first searched for variants able to segregate the disease phenotypes (severe and not-
153 severe) by analyzing a large panel of mutational events (mutations in isoforms, splicing sites,
154 small and long noncoding genes, promoters, TSS, predicted pathogenic mutations, loss of
155 function mutations, among others). We could not find one single mutation or combinations of
156 mutations that were able to completely segregate the two groups (**Supplementary**
157 **Information**) although partial segregation can be observed (**Suppl. Table 2**). As already
158 described for monogenic diseases (Kousi and Katsanis 2015) and cancer (Castro-Giner,
159 Ratcliffe, and Tomlinson 2015), we hypothesized that distinct weak disease-promoting
160 effects may represent patient-specific causes to CMS severity, which bring damage to sets of
161 genes that are functionally related. To find these causes, we sought to search for variants with
162 the potential to alter gene functions, such as CNVs and compound heterozygous variants,
163 which have been previously reported to be key to CMS (Angela Abicht, Müller, and
164 Lochmüller 1993; Richard et al. 2003; Bevilacqua et al. 2017; Yang et al. 2018).

165 ***Compound heterozygous variants are functionally related***

166 In order to explore the hypothesis that disease severity in this cohort is due to variants in
167 patient-specific critical elements, we sought to identify potentially damaging compound
168 heterozygous variants and CNVs. We analyzed the gene lists associated with these mutations
169 to search for evidence of alterations in relevant pathways for the severe (n=8) and not-severe
170 cases (n=12). We first performed a functional enrichment analysis (Methods) of the genes
171 with CNVs found in the two groups. The set of affected genes in the severe group is
172 composed of 26 unique genes (10 private to the severe group), while the not-severe group
173 presented 86 unique genes (**Suppl. Table 3**). None of these gene sets showed any functional
174 enrichment. Moreover, none of these genes had been described as causal for CMS, and none
175 carried compound heterozygous variants. (**Suppl. Figure 2**).

176 As for compound heterozygous variants, the set of affected genes in the severe group is
177 composed of 112 unique genes (89 private to the severe group), while the not-severe group
178 resulted in 152 unique genes (**Suppl. Table 3**). We found that the severe group shows
179 significant enrichment in genes belonging to extracellular matrix (ECM) pathways, in
180 particular “ECM receptor interactions” (KEGG hsa04512, adjusted p-value 0.002337) and
181 “ECM proteoglycans” (Reactome R-HSA-30001787, adjusted p-value 0.001237), which are

182 the top-hit pathways when the 89 genes appearing only in the severe group are considered.
183 Both these pathways share common genes, namely *TNXB*, *LAMA2*, *TNC*, and *AGRN*. The
184 role of extracellular matrix proteins for the formation and maintenance of the NMJ has
185 recently drawn attention to the study of CMS (Beeson 2016; Rodríguez Cruz, Palace, and
186 Beeson 2018). In particular, within the genes linked with ECM pathways, *AGRN* and *LAMA2*
187 stand out for their implication in CMS and other rare neuromuscular diseases (Bertini et al.
188 2011; Nicole et al. 2014; Bönnemann et al. 2014). ECM-related pathways are not enriched in
189 the not-severe set of genes (KEGG hsa04512, adjusted p-value 0.6170). Moreover, top-hit
190 pathways of the not-severe set of genes are not explicitly related to ECM and not consistent
191 between Reactome and KEGG (Reactome “Susceptibility to colorectal cancer” R-HSA-
192 5083636, adjusted p-value 4.131e-7, genes MUC3A/5B/12/16/17/19; KEGG “Huntington’s
193 disease” hsa05016, adjusted p-value 0.07103, genes REST, CREB3L4, CLTCL1,
194 DNAH2/8/10/11). These findings support our hypothesis that the severe patients might
195 present disruptions in NMJ functionally related genes that, combined with *CHRNE* causative
196 alteration, may be responsible for the worsening of symptoms.

197 ***CMS-specific monolayer and multilayer community detection***

198 As disease-related genes tend to be interconnected (Menche et al. 2015), we sought to
199 analyze the relationships among the CMS linked genes (i.e. known CMS causal genes, and
200 severe and not-severe compound heterozygous variants and CNVs; Methods) using network
201 community clustering analysis. We employed the Louvain algorithm (Methods) to find
202 groups of interrelated genes in three monolayer networks that represents biological
203 knowledge contained in databases, separately: the Reactome database (Fabregat et al. 2018),
204 the Recon3D Virtual Metabolic Human database (Brunk et al. 2018) (both downloaded in
205 May 2018), and from the Integrated Interaction Database (IID) (Kotlyar et al. 2016)
206 (downloaded in October 2018) (**Suppl. Figure 3**). The last two networks, represent the
207 ‘metabolome’ and the ‘interactome’ data, respectively. By measuring community similarity
208 (Methods), we observed that the same CMS linked genes did not form the same communities
209 across the different networks (**Suppl. Figure 4**). These results show that, although disease-
210 related genes are prone to form well-defined communities in distinct networks (Goh et al.
211 2007; Cantini et al. 2015), different facets of biological information (i.e. reactome,
212 metabolome, interactome) reflect diverse participation modalities of such genes into
213 communities. In order to deliver an integrated analysis of such heterogeneous information,
214 we further consider them as a multilayer network (Gosak et al. 2018).

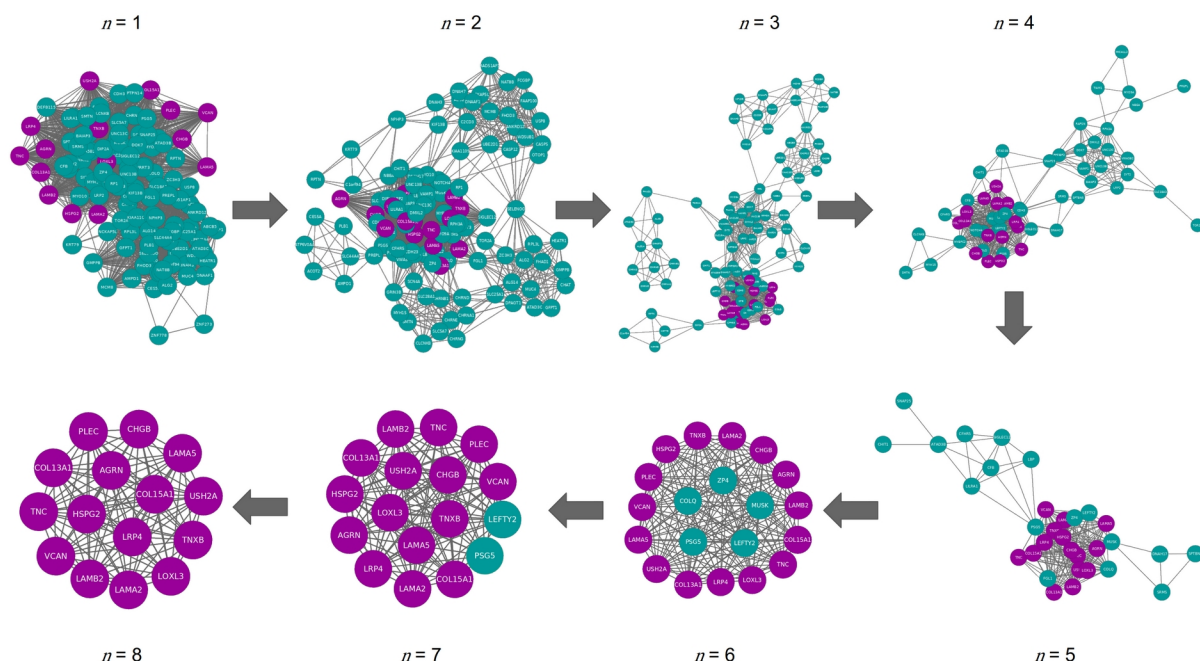
215 ***Large-scale multilayer community detection of disease associated genes***

216 We first sought to test the hypothesis that disease-related genes tend to be part of the same
217 communities also in a multilayer network. We used the curated gene-disease associations
218 database DisGeNET (Piñero et al. 2017), showing that disease-associated genes are
219 significantly found to be members of the same multilayer communities (Wilcoxon test p-
220 value < 0.001 in a range of resolution parameters described in the Methods). We pre-
221 processed DisGeNET database by filtering out diseases and disease groups with only one

222 associated gene (6,352 diseases), and those whose number of associated genes was more than
223 $1.5 \times$ interquartile range (IQR) of the gene associated per disease distribution (823 diseases
224 with more than 33 associated genes) (**Suppl. Figure 5A-B**). This procedure prevents a
225 possible analytical bias due to the higher amounts of genes annotated to specific disease
226 groups (e.g. entry C4020899, “Autosomal recessive predisposition”, annotates 1445 genes).
227 We then retrieved the communities of each associated gene, excluding 428 genes not present
228 in our multilayer network and the diseases left with only one associated gene. The final
229 analysis comprised a total of 5,892 diseases with an average number of 7.38 genes per
230 disease. For each disease, we counted the number of times that the disease-associated genes
231 are found in the same multilayer communities, and compared the distribution of such
232 frequencies with that of balanced random associations (1000 randomizations). Results show
233 that disease-associated genes are significantly found in the same multilayer communities
234 across the resolution interval (**Suppl. Figure 5C**).

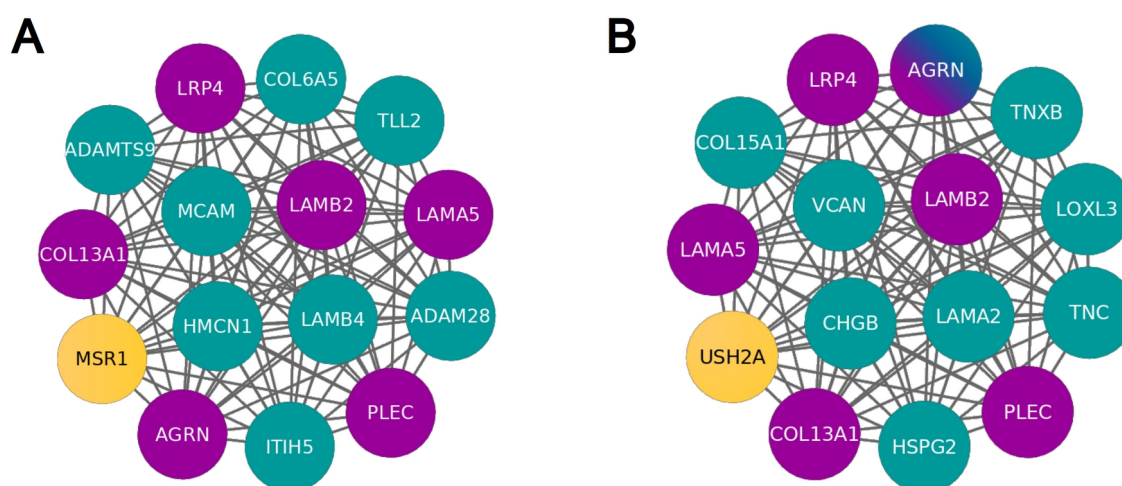
235 *Modules within the CMS multilayer communities*

236 We define a module as a group of CMS linked genes that are systematically found to be part
237 of the same multilayer community while increasing the multilayer network community
238 resolution parameter (Methods; Supplementary Information; **Figures 3-4**).



239 **Figure 3.** Identification of the largest module containing genes that are found in the same community
240 in the entire range of resolution parameters (Methods). In each module, genes are connected if they
241 are found in the same multilayer communities at n values of the resolution parameter γ within the
242 range under consideration ($\gamma \in (0,4]$). The arrows indicate the systematic increase of n . At $n = 8$, the
243 module contains genes that are always found in the same community in the entire range of resolution
244 (see Supplementary Information "Multilayer community detection analysis"). The largest modules
245 containing the CMS linked gene set (highlighted in pink), which includes known CMS causal genes,
246 severe-specific heterozygous compound variants and CNVs, are shown.

247 Within each of these communities, we identified smaller modules of CMS linked genes that
248 are specific to the severe and not-severe groups. We tested the significance of obtaining these
249 exact genes in the severe and not-severe largest modules upon severity class label shuffling
250 among all individuals (1000 randomizations). We found that 13 (p-value 0.034; on average 8
251 CMS linked genes and 5 causal genes) and 14 (p-value 0.026; on average 8 CMS linked
252 genes and 4 causal genes) are the minimum number of genes composing the modules that are
253 not expected to be found at random in the severe and not-severe largest components,
254 respectively (**Suppl. Figure 6**). In the two groups, the significantly largest module that
255 contains known CMS causal genes is composed of 15 genes (**Figure 4**). 6 out of these 15 are
256 previously described CMS causal genes (Methods), namely the ECM heparan sulfate
257 proteoglycan agrin (*AGRN*); the cytoskeleton component plectin (*PLEC*), causative of
258 myasthenic disease (Forrest et al. 2010); the agrin receptor *LRP4*, key for AChR clustering at
259 NMJ (Barik et al. 2014) and causative of CMS by compound heterozygous variants
260 (Ohkawara et al. 2014); the ECM components *LAMA5* and *LAMB2* laminins, and *COL13A1*
261 collagen.



262 **Figure 4.** Largest module, containing known CMS causal genes, within the multilayer communities
263 of CMS linked genes that are specific to the not-severe (A) and severe (B) groups. In turquoise,
264 compound heterozygous variants; in yellow, CNVs; in pink, known CMS causal genes. Being a CMS
265 causal gene bearing compound heterozygous variants, *AGRN* is depicted using both turquoise and
266 pink.

267 All the other genes of the two modules are involved in a varied spectrum of muscular
268 dysfunctions, discussed in the following sections. As the location of the causal gene products
269 determine the most common classification of the disease (i.e. presynaptic, synaptic, and
270 postsynaptic CMS) (Rodríguez Cruz, Palace, and Beeson 2018), we determined class and
271 localization of the members of the found modules (**Table 2**). Laminins, well-known CMS
272 glycoproteins, are affected in both severe (*LAMA2*, *USH2A*) and not-severe (*LAMB4*) groups,
273 and are bound by specific receptors that are damaged in the not-severe group (*MCAM*)

274 (Dagur and McCoy 2015). Collagens, known CMS-related factors, are associated with the
275 not-severe group (*COL6A5*), and bound by specific receptors that are damaged in the not-
276 severe group (*MSR1*) (Gowen et al. 2000).

277 However, overall collagen biosynthesis is affected in both severe and not-severe groups.
278 Indeed, metalloproteinases, damaged in the not-severe group, are responsible for the
279 proteolytic processing of lysyl oxidases (*LOXL3*), which are implicated in collagen
280 biosynthesis (Panchenko et al. 1996) and damaged in the severe group.

281 Alterations in proteoglycans (*AGRN*, *HSPG2*, *VCAN*, *COL15A1*) (Iozzo and Schaefer 2015),
282 tenascins (*TNC*, *TNXB*) (Pedrosa-Domellöf, Virtanen, and Thornell 1995), and
283 chromogranins (*CHGB*) (Andreose, Sala, and Fumagalli 1994) are specific of the severe
284 group. We observed no genes associated with proteoglycan damage in the not-severe group,
285 suggesting a direct involvement of ECM in CMS severity.

286 ***Personalized analysis of the severe cases***

287 We sought to analyze the 15 genes of the largest module of the severe group in each one of
288 the 8 patients, hereafter referred to using the WGS sample labels (**Suppl. Table 1**). Overall,
289 these genes have a varied range of expression levels in tissues of interest (**Suppl. Figure 7**),
290 for instance in skeletal muscle *HSPG2*, *LAMA2*, *PLEC* and *LAMB2* show medium expression
291 levels (9 to 107 TPM) while the others show low expression levels (0.6 to 9 TPM) (Methods).
292 Patient 2, a 15 years old male, presents compound heterozygous variants in tenascin C (*TNC*),
293 mediating acute ECM response in muscle damage (Sorensen et al. 2018), and CNVs
294 (specifically, a partial heterozygous copy number loss) in usherin (*USH2A*), which has been
295 associated with hearing and vision loss (Austin-Tse et al. 2018).

296 Patient 16, a 25 years old female, presents compound variants in tenascin XB (*TNXB*), which
297 is mutated in Ehlers-Danlos syndrome, a disease that has already been reported to have
298 phenotypic overlap with muscle weakness (Kirschner et al. 2005; N. C. Voermans and van
299 Engelen 2008) and whose compound heterozygous variants have been reported for a primary
300 myopathy case (Pénisson-Besnier et al. 2013; Nicol C. Voermans et al. 2014); and versican
301 (*VCAN*), which has been suggested to modify tenascin C expression (Keller et al. 2012) and
302 is upregulated in Duchenne muscular dystrophy mouse models (McRae et al. 2017).

303 Patient 13, a 26 years old male, presents compound mutations in laminin $\alpha 2$ chain (*LAMA2*),
304 a previously reported gene related to various muscle disorders (Amin et al. 2019; Løkken et
305 al. 2015, 2; Dimova and Kremensky 2018, 2) whose mutations cause reduction of
306 neuromuscular junction folds (Rogers and Nishimune 2017), and collagen type XV α chain
307 (*COL15A1*), which is involved in guiding motor axon development (Guillon, Bretaud, and
308 Ruggiero 2016) and functionally linked to a skeletal muscle myopathy (Eklund et al. 2001;
309 Muona et al. 2002).

310 Patient 12, a 49 years old female, presents compound mutations in chromogranin B4
311 (*CHGB*), potentially associated with amyotrophic lateral sclerosis early onset (Pampalakis et
312 al. 2019). Patient 18, a 51 years old man, presents compound mutations in agrin (*AGRN*), a
313 CMS causal gene that mediates AChR clustering in the skeletal fiber membrane (Huzé et al.
314 2009).

Activity localization	Class	CMS causal gene	Phenotype group		Function	Synaptic localization (Manual curation)	Localization (UniProt)
			Not-severe	Severe			
ECM (ECM)	Proteoglycans	AGRN	-	AGRN	Cell hydration and growth factor trapping	Pre- and postsynaptic (PMID: 29462312)	Synaptic basal lamina / ECM
		-	-	HSPG2		Basement membrane (PMID:30453502)	Basement membrane / ECM
		-	-	VCAN		ECM (PMID:29211034)	ECM
		-	-	COL15A1		Basement membrane (PMID:26937007)	ECM
	Collagens	COL13A1	-	-	Structural support	Basement membrane, post-synaptic (PMID: 30768864)	Post-synaptic cell membrane
		-	COL6A5	-		Basement membrane (PMID:23869615)	Extracellular matrix
	Laminins	LAMA5	-	-	Web-like structures	Pre-synaptic (PMID:28544784)	Basement membrane / ECM
		LAMB2	-	-		Basement membrane (PMID:27614294)	Basement membrane / ECM / Synaptic cleft
		-	LAMB4	-		Myenteric plexus basement membrane (PMID: 28595269)	Basement membrane / ECM
		-	-	LAMA2		Pre-synaptic (PMID:9396756)	Basement membrane / ECM
		-	-	USH2A		Neuronal projection of stereocilia (PMID:19023448)	Stereocilia membrane / Secreted (Extracellular region)
	Fibulins	-	HMCN1	-	Scaffolding	Glomerular Extracellular matrix (PMID: 29488390)	Basement membrane / ECM
	Tenascins	-	-	TNC	Anti-adhesion	Basement membrane (PMID: 29466693)	ECM / Perisynaptic ECM (Ensembl)
				TNXB		Basement membrane (PMID: 23768946)	ECM
	Enzymes	-	-	LOXL3	Collagen assembly	Basement membrane (PMID:26954549)	Secreted (extracellular region)

			ADAMTS9	-	Proteoglycan cleavage	Secreted to ECM (PMID:30626608)	ECM	
			ADAM28			ECM (PMID:24613731)	Cell membrane / Secreted (extracellular region)	
		Neuropeptides	-	-	CHGB	Regulatory peptides precursor	Pre- and postsynaptic (PMID:7526287)	Secreted (extracellular region)
		Others	-	ITIH5	-	Hyaluronic acid binding	ECM (PMID:27143355)	Secreted (extracellular region)
Cell surface	Receptors		MSR1	-	Proteoglycan and collagen binding	Macrophage surface Scavenger Receptor (PMID:12488451)	Plasma membrane	
			MCAM			Plasma membrane (PMID:28923978)	Plasma membrane	
			LRP4	-	-	Laminin binding	Post-synaptic (PMID:25319686)	Post-synaptic cell membrane
Cytoplasm	Cytoskeleton		PLEC	-	Structural support	Post-synaptic (PMID:20624679)	Post-synaptic cytoskeleton	

315 **Table 2.** Localization and functions of proteins encoded by the genes found in the largest modules of
316 the multilayer communities of severe and not-severe groups. In turquoise, compound heterozygous
317 variants; in yellow, CNVs; in pink, known CMS causal genes. Synaptic localization was retrieved
318 from manual curation and Uniprot database (Methods).

319 Patient 20, a 57 years old male, presents compound mutations in lysyl oxidase-like 3
320 (*LOXL3*), involved in myofiber extracellular matrix development by improving integrin
321 signaling through fibronectin oxidation and interaction with laminins (Kraft-Sheleg et al.
322 2016), and perlecan (*HSPG2*), a gene whose deficiency leads to muscular hypertrophy (Xu et
323 al. 2010), that is also mutated in Schwartz-Jampel syndrome (Stum et al. 2006),
324 Dyssegmental dysplasia Silverman-Handmaker type (*DDSH*) (Arikawa-Hirasawa et al. 2002)
325 and fibrosis (Lord et al. 2018), such as Patient 19, a 62 years old female. Furthermore, based
326 on the estimated familial relatedness (Methods) and personal communication (February 2018,
327 Teodora Chamova), patients 19 and 20 are siblings (**Suppl. Table 4**).

328 **Functional consequences of variants in the severe-specific module**

329 Studying the functional impact of the compound heterozygous variants in the severe-specific
330 genes of the module, we observed that **in 6 of the 8 patients at least one of the variants is**
331 **predicted to be deleterious by the Ensembl Variant Effect Predictor (VEP)** (McLaren et
332 al. 2016) (Methods; **Suppl. Table 5**). For example, as for Patient 18, who presents 3 different
333 variants in *AGRN* gene, only rs200607541 is predicted to be deleterious by VEP's Condel
334 (score = 0.756), SIFT (score = 0.02), and PolyPhen (score = 0.925).

335 In particular, the variant (a C>T transition) presents an allele frequency (AF) of 4.56E-03
336 (gnomAD exomes) (Karczewski et al. 2020) and affects a region encoding a position related
337 to a EGF-like domain (SMART:SM00181) and a Follistatin-N-terminal like domain
338 (SMART:SM00274). Both of these domains are part of the Kazal domain superfamily which
339 are specially found in the extracellular part of agrins (PFAM: CL0005) (Laskowski and Kato
340 1980). On the other hand, Patient 16 presents a total of 38 *TNXB* transcripts affected by three
341 gene variants (rs201510617, rs144415985, rs367685759) that are all predicted to be
342 deleterious by the three scoring systems, have allele frequencies of 3.17E-02, 4.83E-02 and
343 5.90E-03, respectively; and in overall, are affecting two conserved domains. The first consists
344 of a fibrinogen related domain that is present in most types of tenascins (SMART:SM00186),
345 while the second is a fibronectin type 3 domain (SMART:SM00060) that is found in various
346 animal protein families such as muscle proteins and extracellular-matrix molecules (Bork and
347 Doolittle 1992). Two of the severe patients (Patients 12 and 19) present severe-only specific
348 compound heterozygous variants that are not predicted to be deleterious. However, one
349 variant in the *CHGB* gene (rs742710, AF=1.07E-01), present in patient 12, has been
350 previously reported to be potentially causative for amyotrophic lateral sclerosis early onset
351 (Pampalakis et al. 2019). This gene has also been strongly suggested in literature as a
352 possible marker for multiple sclerosis (Mo et al. 2013), and other related neural diseases like
353 Parkinson's (Nilsson et al. 2009) and Alzheimer's disease (Y. Chen et al. 2019). As for
354 patient 19, the variant rs146309392 (AF=8.40E-04) in the gene *HSPG2* has been previously
355 referred to be causal of Dyssegmental dysplasia as a compound heterozygous mutation
356 (Arikawa-Hirasawa et al. 2001). This variant, as pointed out before, is shared with sibling
357 patient 20. One severe individual (Patient 3), a 37 years old female, does not carry compound
358 heterozygous variants included in this module but others at a lower resolution parameter
359 value (**Suppl. Figure 8; Suppl. Table 6**). Interestingly, most of the genes carrying severe-
360 specific deleterious compound heterozygous variants in this patient (*CDH3*, *FAAP100*,
361 *FCGBP*, *GFY*, *RPTN*) are not related to processes at the NMJ level (Hull et al. 2016;
362 Ramanagoudr-Bhojappa et al. 2018; Johansson, Thomsson, and Hansson 2009; Swuec et al.
363 2017; Kaneko-Goto et al. 2013). Nevertheless, three of these variants occur in genes
364 potentially involved in NMJ functionality. In particular, variants rs111709242 (AF=2.64E-
365 03) and rs77975665 (AF=3.03E-02) affect gene *PPFIBP2*, which encodes a member of the
366 liprin family (liprin- β) that has been described to control synapse formation and postsynaptic
367 element development (Bernadzki et al. 2017; Astigarraga et al. 2010). Furthermore, the
368 variant rs111709242 is predicted to be deleterious by the SIFT algorithm (see **Suppl. Table**
369 **6**). Moreover, variant rs151154986 (AF=2.18E-02) affects the acyl-CoA thioesterase *ACOT2*,
370 which generate CoA and free fatty acids from acyl-CoA esters in peroxisomes (Grevengoed,
371 Klett, and Coleman 2014). A role for CoA levels in skeletal muscle for this enzyme class has
372 been previously described (Li et al. 2015). Interestingly, *PPFIBP2* appears in modules at
373 lower resolution parameter values associated with known CMS causal genes (e.g. *DOK7*,
374 *RPSN*, *RPH3A*, *VAMP1*, *UNC13B*). Moreover, this patient presents high relatedness with
375 three not-severe patients (Patients 8, 9, and 10) who in turn display a very high relatedness
376 among them (**Suppl. Table 4**).

377 **Potential pharmacological implications**

378 Finding a genetic diagnosis might help select the appropriate medication for each patient. For
379 instance, fluoxetine and quinine are used for treating the slow-channel syndrome, an
380 autosomal dominant type of CMS caused by mutations affecting the ligand binding or pore
381 domains of AChR, but this treatment should be avoided in patients with fast-channel CMS
382 (Engel et al. 2015).

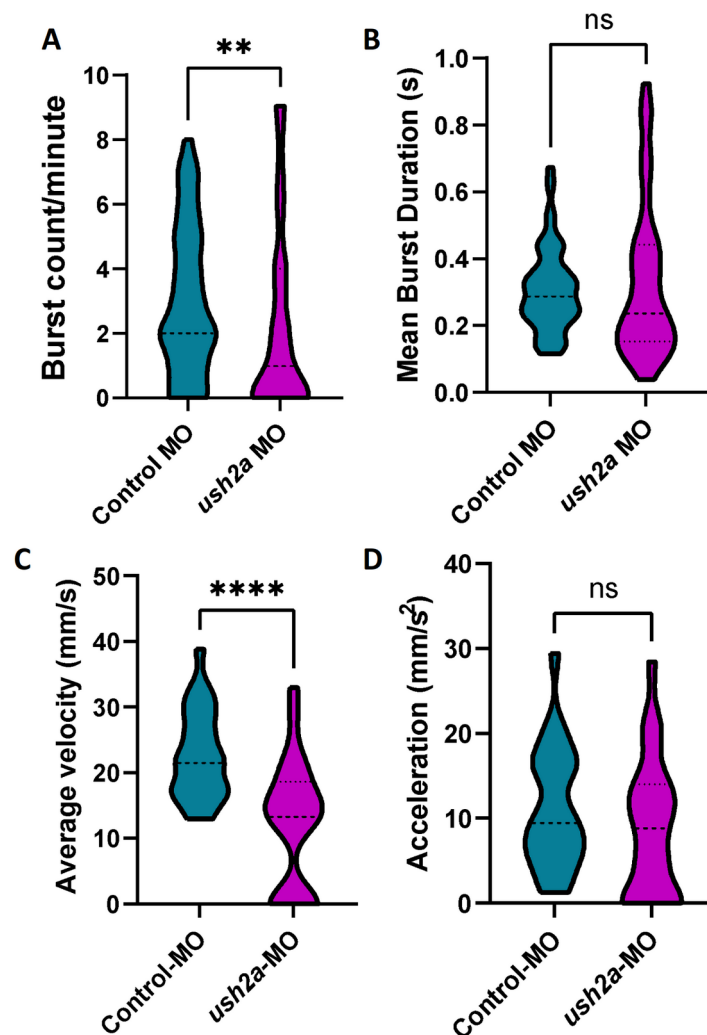
383 Within our cohort, 13 (7 mild, 2 moderate and 4 severe) out of 20 individuals from our CMS
384 cohort are receiving a pharmacological treatment consisting of pyridostigmine, an
385 acetylcholinesterase inhibitor used to treat muscle weakness in myasthenia gravis and CMS
386 (Lee, Beeson, and Palace 2018). This treatment slows down acetylcholine hydrolysis,
387 elevating acetylcholine levels at the NMJ, which eventually extends the synaptic process
388 duration when the AChR are mutated. Although the severity could potentially be related to
389 how well a patient responds to the standard treatment with the AchE inhibitors, we could not
390 find a clear correlation between severity and pyridostigmine treatment (two-tailed Fisher's
391 exact test p-value 0.356; **Suppl. Figure 1**).

392 In Addition to the causal mutation in *CHRNE*, our results indicate that severity is related to
393 AChR clustering at the Agrin-Plectin-LRP4-Laminins axis level, suggesting the potential
394 benefit of pharmaceutical intervention enhancing the downstream process of AChR
395 clustering. For example, beta-2 adrenergic receptor agonists like ephedrine and salbutamol
396 have been documented as capable of enhancing AChR clustering (Clausen, Cossins, and
397 Beeson 2018) and proved to be successful in the treatment for severe AChR deficiency
398 syndromes (Rodríguez Cruz et al. 2015) (Garg and Goyal, 2022). Furthermore, the addition
399 of salbutamol in pyridostigmine treatments have been described as being able to ameliorate
400 the possible secondary effects of pyridostigmine in the postsynaptic structure
401 (Vanhaesebrouck et al. 2019).

402 **Experimental validation of *USH2A* involvement at the NMJ**

403 To determine the potential relevance of one of our identified potential modifiers with no
404 previously published relationship to the NMJ, we analyzed its function using zebrafish. For
405 this we chose *USH2A*, a gene associated with Usher syndrome and Retinitis pigmentosa in
406 humans (OMIM ID 608400, <https://omim.org/>), which was identified as a copy number loss
407 in patient 2. While we expect the phenotypic outcome (more severe disease) of this genetic
408 difference to manifest when expressed in conjunction with the *CHRNE* mutation causing this
409 patients' CMS, we hypothesized that knockdown of *USH2A* expression alone may cause
410 detectable NMJ impairments. Therefore, we used a MO to knockdown the expression of the
411 zebrafish orthologue; *ush2a*, and studied the effects on survival, development and NMJ
412 function. Zebrafish *ush2a* is expressed from 1 to 5 dpf, as shown in **Suppl. Figure 9A**. Using
413 a MO targeting the exon 3/intron 3 splice donor site we were able to decrease expression of
414 *ush2a* with a 6 ng to 18 ng MO injection (**Suppl. Figure 9B**). Survival of control and *ush2a*-
415 MO zebrafish was not significantly affected as compared to wildtype (WT) fish over 5 dpf
416 (log-rank test, WT n = 574, control MO 4 ng n = 46, 6 ng n = 75, 18 ng n = 34, *ush2a*-MO 2
417 ng n = 72, 4 ng n = 68, 6 ng n = 360, 12 ng n = 288, 18 ng n = 139, **Suppl. Figure 9C**).

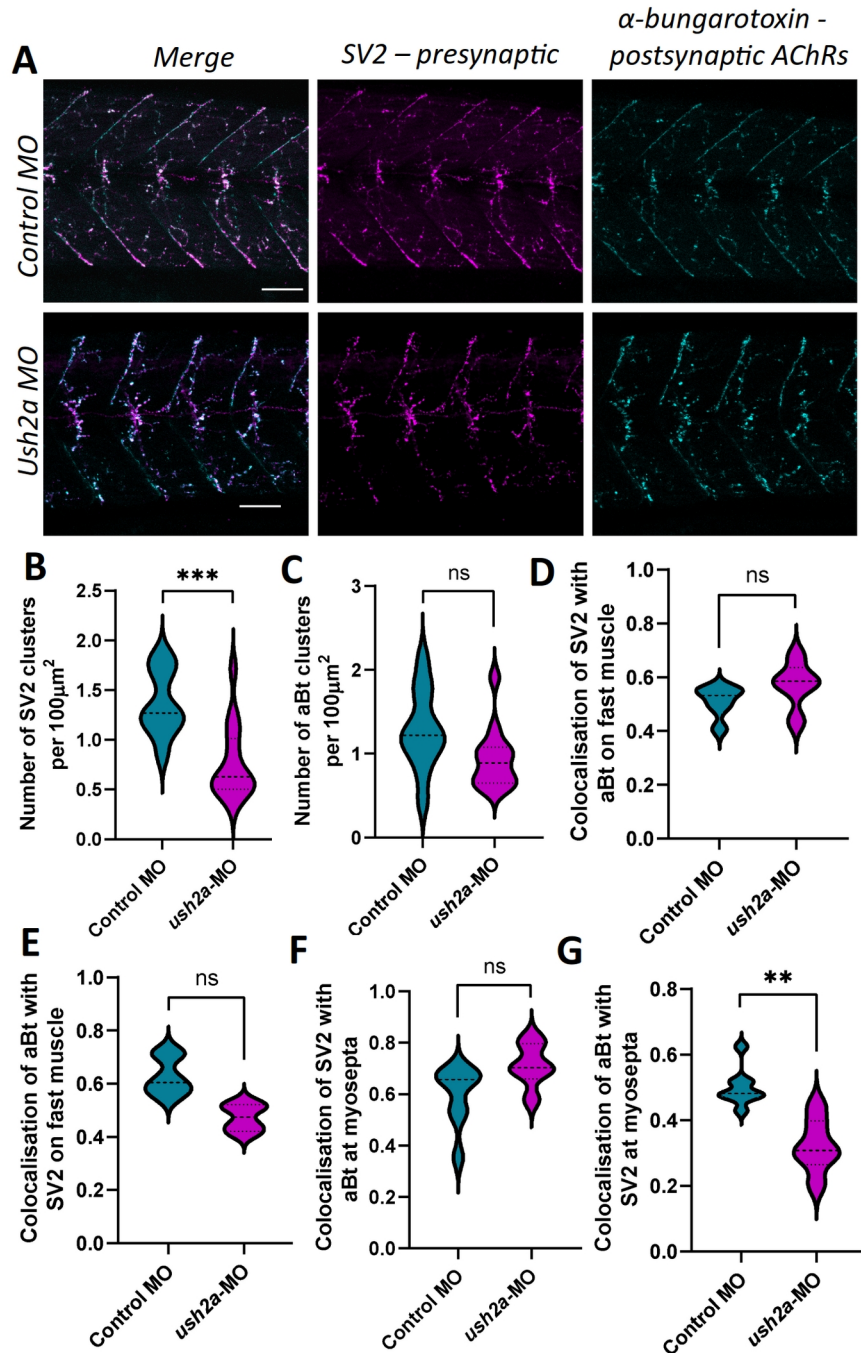
418 There were no obvious gross morphological differences between control MO and *ush2a*-MO
419 fish up to 5 dpf (representative images of 2 dpf fish shown in **Suppl. Figure 9D**). As length
420 is an indicator of developmental stage, we measured the length of 18 ng injected *ush2a*-MO
421 fish at 2 dpf and found a significant reduction in length as compared to controls ($p = 0.013$, t
422 $= 2.59$, $df = 38$, unpaired t-test, control MO $n = 20$, *ush2a*-MO $n = 20$, **Suppl. Figure 9E**).
423 Eye area can be reduced in zebrafish models of retinitis pigmentosa, the condition that
424 *USH2A* mutations are associated with in humans. We measured eye area in 2 dpf fish and
425 found it to be significantly reduced in 18 ng-injected *ush2a*-MO fish as compared to controls
426 ($p = 0.0006$, $t = 3.73$ $df = 38$, unpaired t-test, control MO $n = 20$, *ush2a*-MO $n = 20$,
427 **Supplementary Figure 9F**).



428 **Figure 5.** Early movement behaviors in *ush2a*-MO zebrafish. (A) Chorion rotations per minute (burst
429 count), and (B) mean chorion rotation duration in seconds for control and *ush2a*-MO-injected
430 zebrafish at 1 days post fertilization (dpf). (C) Average velocity and (D) initial acceleration of control
431 and *ush2a*-MO zebrafish at 2 dpf in response to touch. Dashed line shows the median, dotted lines
432 show the quartiles, ** $p < 0.01$, **** $p < 0.0001$, ns = not significant, Mann Whitney test (A and B),
433 unpaired t-test (C and D).

434 Eye area remains significantly different after normalizing for body length (data not shown).
435 CMS manifests as fatigable muscle weakness in patients and in developing zebrafish we can
436 study the ability of fish to perform repetitive, well-characterized movements during
437 development to determine whether impairments to the functioning of the neuromuscular
438 system may be present. We quantified the number and duration of chorion movements in 1
439 dpf fish following administration of a control or 18 ng *ush2a*-MO. This revealed a significant
440 decrease in the number of burst events performed per minute in knockdown fish as compared
441 to controls ($p = 0.003$, Mann Whitney test, control MO $n = 84$, *ush2a*-MO $n = 74$, **Figure**
442 **5A**). The average duration of each burst event was not significantly affected by loss of Ush2a
443 ($p = 0.467$, Mann Whitney test, control MO $n = 72$, *ush2a*-MO $n = 49$, **Figure 5B**). To
444 ascertain whether impairments to movement are present in the knockdown fish while
445 swimming free of the chorion, we also performed a touch response assay at 2 dpf. We
446 observed a significant decrease in average velocity of the fish injected with *ush2a*-MO as
447 compared to control MO in response to a touch stimulus ($p < 0.0001$, $t = 4.42$, $df = 48$,
448 unpaired t-test; $n = 25$, **Figure 5C**). There was no significant difference in acceleration of
449 *ush2a*-MO fish as compared to controls ($p = 0.263$, $t = 1.13$ $df = 47$, unpaired t-test; control
450 MO $n = 24$, *ush2a*-MO $n = 25$, **Figure 5D**).

451 To determine whether changes in movement are reflected at the level of gross NMJ structure,
452 analysis of NMJ morphology was performed on 2 dpf zebrafish (**Figure 6A**). A significant
453 decrease in the number of SV2-positive clusters per $100 \mu\text{m}^2$ (representative of the pre-
454 synaptic motor neurons) was identified on the fast muscle fibers of *ush2a*-MO fish as
455 compared to controls ($p = 0.0004$, Mann Whitney test, control MO $n = 11$, *ush2a*-MO $n = 15$,
456 **Figure 6B**). SV2-positive clusters overlie postsynaptic AChRs to form NMJs and these
457 receptors can be detected with fluorophore-labelled α -bungarotoxin. Analysis of AChR
458 clusters revealed no significant differences in number per $100 \mu\text{m}^2$ between the two
459 conditions ($p = 0.217$, Mann Whitney test, control MO $n = 11$, *ush2a*-MO $n = 15$, **Figure**
460 **6C**). Colocalization analysis revealed no significant differences in co-occurrence of SV2 and
461 AChR on fast muscle fibers (SV2 colocalization with AChRs: $p = 0.371$, $t = 0.911$, $df = 24$,
462 nested t-test, **Figure 6D** and AChR colocalization with SV2: $p = 0.372$, $t = 0.909$, $df = 24$,
463 control MO $n = 11$, *ush2a*-MO $n = 15$, nested t-test, **Figure 6E**). There was also no
464 significant difference in colocalization of SV2 with AChRs on slow muscle, however, a
465 significant reduction in co-occurrence of AChRs with SV2 is present on *ush2a*-MO slow
466 muscle (SV2 colocalization with AChRs: $p = 0.516$, $t = 0.660$, $df = 24$, nested t-test, **Figure**
467 **6F** and AChR colocalization with SV2: $p = 0.002$, $t = 3.41$, $df = 24$, control MO $n = 11$,
468 *ush2a*-MO $n = 15$, nested t-test, **Figure 6G**). Movement differences in zebrafish may also be
469 caused by changes in muscle growth and development. Therefore, we assessed 2 dpf fish for
470 gross phenotypic differences in muscle fiber orientation and structure using a phalloidin stain
471 to detect actin in muscles (**Suppl. Figure 10A**). We identified no significant differences in
472 muscle fiber dispersion (organization) or myotome size between *ush2a*-MO and control-MO
473 zebrafish ($p = 0.922$, $t = 0.099$, $df = 24$ unpaired t-test and $p = 0.985$, $t = 0.019$, $df = 24$ nested
474 t-test, respectively. Control MO $n = 11$ and *ush2a*-MO $n = 15$, **Suppl. Figure 10B, C**).



475 **Figure 6.** Neuromuscular junction morphology in *ush2a*-MO zebrafish. (A) Representative images of
 476 neuromuscular junctions from control and *ush2a*-MO zebrafish at 2 days post fertilization (dpf).
 477 Acetylcholine receptors (AChRs) are stained with fluorophore bound α -bungarotoxin (aBt, cyan), and
 478 motor neurons detected with an antibody against synaptic vesicle protein 2 (SV2, magenta). Scale bar
 479 = 50 μm . (B) Number of SV2-positive clusters and (C) number of aBt-positive clusters per 100 μm^2 .
 480 (D) Colocalization of SV2 with aBt and (E) colocalization of α BT with SV2 on fast muscle cells,
 481 using Mander's correlation coefficient (0 = no colocalization, 1 = full colocalization). (F)
 482 Colocalization of SV2 with aBt and (G) colocalization of aBt with SV2 on slow muscle cells at the
 483 myosepta, using Mander's correlation coefficient. Dashed line shows the median, dotted lines show
 484 the quartiles, **p < 0.05, ***p < 0.001, ns = not significant, nested t-test.

485 Discussion

486 In this work, we have developed a framework for the analysis of disease severity in scenarios
487 heavily impacted by sample size. Presenting limited numbers of cases is one of the main
488 obstacles for the application of precision medicine methods in rare disease research, as it
489 critically affects the level of expected statistical power, a common hallmark in the analysis of
490 minority conditions (Whicher, Philbin, and Aronson 2018). This fact difficults exploring the
491 molecular relationships that define the inherently heterogeneous levels of disease severity
492 observed in rare disease populations, making it an atypically addressed biomedical problem
493 (Boycott et al. 2013). Our approach, based on the application of multilayer networks, enable
494 the user to account for the many interdependencies that are not properly captured by a single
495 source of information, effectively combining the available patient genomic information with
496 general biomedical knowledge from relevant databases representing different aspects of
497 molecular biology. The application to a relevant clinical case, where we tested the hypothesis
498 that the severity of CMS is determined by patient-specific alterations that impact NMJ
499 functionality, provided evidence on how the methodology is able to recover the molecular
500 relationships between the candidate patient-specific genomic variants, the observed causal
501 AChR mutation and previously described CMS causal genes (**Table 1**).

502 Our in-depth functional analysis focused on a cohort of 20 CMS patients, from a narrow,
503 geographically isolated and ethnically homogenous population, who share the same causative
504 mutation in the AChR ϵ subunit (CHRNE) but present with different levels of severity. The
505 isolation and endogamy that characterize the population from which these patients come from
506 might have favored the accumulation of damaging variants (Fareed and Afzal 2017;
507 Petukhova et al. 2009), giving rise to the emergence of compound effects on relevant genes
508 for CMS. This observation has previously been made in similar syndromes (Ohno 2003;
509 Müller et al. 2004) and in a number of other neuromuscular diseases (Zhong et al. 2017;
510 Wang et al. 2018). In CMS, compound heterozygous variants are known to be concentrated
511 in CHRNE (Thompson et al. 2019). The initial analysis of compound heterozygous variants
512 revealed a significant enrichment of functional categories that are specific to the severe cases,
513 namely ECM functions. This suggests the existence of functional relationships between major
514 actors of the NMJ that are affected by severity-associated damaging mutations. Such
515 interactors include already known CMS causal genes (e.g. AGRN, LRP4, PLEC) as well as
516 genes known to interact with them. While severity-specific compound heterozygous variants
517 and CNVs are observed, demographic factors (e.g. sex, age), pharmacological treatment, and
518 personalized omics data (e.g. variant calling, differential gene expression, allele specific
519 expression, splicing isoforms) do not segregate with patient severity.

520 Therefore, this motivated the developing of our multilayer network community analysis to
521 investigate the relationship between known CMS causal genes and severity-associated
522 variants (compound heterozygous variants and CNVs), integrating pathways, metabolic
523 reactions, and protein-protein interactions. Recently, we used a multilayer network as a
524 means to perform dimensionality reduction tasks for patient stratification in
525 medulloblastoma, a childhood brain tumor (Núñez-Carpintero et al. 2021). Here, we started
526 by analyzing DisGeNET data in order to verify that disease-associated genes tend to belong

527 to the same multilayer communities. We then identified stable and significantly large gene
528 modules within our CMS cohort's multilayer communities and mapped the corresponding
529 damaging mutations back to the single patients, providing a personalized mechanistic
530 explanation of severity differences. Given the difficulties of cohort recruitment for rare
531 diseases, this approach could be used to investigate forms of CMS and other phenotypically
532 variable rare diseases caused by a common mutation (Estephan et al. 2018).

533 Overall, the personalized analysis of these mutations suggests that CMS severity can be
534 ascribed to the damage of specific molecular functions of the NMJ which, despite affecting
535 individuals in a personalized manner, involve genes belonging to distinct classes and
536 localizations, namely ECM components (proteoglycans, tenascins, chromogranins) and
537 postsynaptic modulators of AChR clustering (LRP4, PLEC) (Table 2). Alterations of other
538 genes related to the production of ECM components, such as laminins and collagen, are
539 observed but are not specific to the severity levels.

540 Finding a personalized genetic diagnosis for phenotypic severity might help select the
541 appropriate medication for each patient. For instance, fluoxetine and quinine are used for
542 treating the slow-channel syndrome, an autosomal dominant type of CMS caused by
543 mutations affecting the ligand binding or pore domains of AChR, but this treatment should be
544 avoided in patients with fast-channel CMS (Engel et al. 2015). Within our cohort, 13 out of
545 20 individuals from our CMS cohort are receiving a pharmacological treatment consisting of
546 pyridostigmine, an acetylcholinesterase inhibitor used to treat muscle weakness in
547 myasthenia gravis and CMS (Lee, Beeson, and Palace 2018). Although the severity could
548 potentially be related to how well a patient responds to the standard treatment with the AChE
549 inhibitors, we could not find a clear correlation between severity and pyridostigmine
550 treatment (two-tailed Fisher's exact test p-value 0.356; Suppl. Figure 1). Our results indicate
551 that severity is related to AChR clustering at the Agrin-Plectin-LRP4-Laminins axis level,
552 suggesting the potential benefit of pharmaceutical intervention enhancing the downstream
553 process of AChR clustering. Strikingly, beta-2 adrenergic receptor agonists like ephedrine
554 and salbutamol have been documented as capable of enhancing AChR clustering (Clausen,
555 Cossins, and Beeson 2018) and proved to be successful in the treatment for severe AChR
556 deficiency syndromes (Sadeh, Shen and Engel, 2011) (Rodríguez Cruz et al. 2015)
557 (Vanhaesebrouck et al. 2019) (Garg and Goyal, 2022), but a strong molecular explanation for
558 the observed favorable effects was still missing. This study reinforces explainability for the
559 described successful usage of such treatments by relating CMS phenotypic severity with the
560 normal development of AChR clusters at the motor neuron membrane.

561 Several of the genes identified in this analysis do not have previous associations with the
562 NMJ, such as the Usher syndrome and Retinitis pigmentosa associated gene; USH2a,
563 identified as a copy number loss in patient 2. To provide proof of principal for this gene
564 acting as a potential modifier of CMS severity, we investigated whether knockdown of *ush2a*,
565 the zebrafish orthologue, could result in NMJ defects. Both CRISPR and TALEN-mediated
566 knockout of *ush2a* in zebrafish have previously revealed phenotypes consistent with Usher
567 syndrome and Retinitis pigmentosa such as hearing loss and progressive visual impairments
568 (Han et al. 2018).

569 However, neither study assessed impacts on muscle structure or movement of the fish.
570 Zebrafish perform well-characterized movements throughout development, starting with
571 spontaneous chorion rotations from approximately 17 hours post fertilization (hpf, the time at
572 which primary motor axons start extending into the muscle) to 30 hp (Saint-Amant &
573 Drapeau. 1998). We treated 1-cell-stage embryos with a high dose of MO to reduce
574 expression of *ush2a* (or equivalent dose of a control MO) and found a decrease in the number
575 of chorion rotations performed at 24 hpf. These movements are mediated at the level of the
576 spinal cord and are independent of supraspinal inputs (Downes & Granato. 2006), thus
577 implying an early defect in NMJ or muscle development, or in signal transduction in the
578 spinal cord/peripheral nervous system. By 2 dpf zebrafish can respond to touch and do so by
579 rapidly swimming at least 1 body-length away from the stimulus (Saint-Amant & Drapeau.
580 1998). In *ush2a*-MO fish the average swimming velocity was significantly slower than in
581 controls, whereas the initial acceleration (proportional to the force of muscle contraction) was
582 unaffected (Sztal et al 2016). This implies that the initial fast muscle response is not
583 significantly affected at this time-point, but that loss of *Ush2a* at the NMJs of slow muscle
584 may be impacting swimming. Defects in movement are reported in many other zebrafish
585 models of CMS, such as those lacking *Dok7* (Müller et al. 2010), *Gfpt1* (Senderek et al.
586 2011) and *Syt2* (Wen et al. 2010). Our motility findings are supported by the identification of
587 a reduction in colocalization of AChRs with SV2-positive clusters on slow muscle fibers in 2
588 dpf fish, thus showing an increase in the number of AChRs that have not been contacted by a
589 motor axon. We also identified an overall reduction in the number of SV2-positive clusters,
590 which may be indicative of a defect or delay in development of the motor nervous system.
591 Previous studies have commented on *USH2A* presence on the basement membranes of
592 perineurium nerve fibers (Pearsall et al. 2002) (Schwaller et al. 2021), however, further
593 functional studies will be required to determine the precise localization of the defect and
594 whether loss of *USH2a* alone can impact NMJ signaling or whether co-occurrence with
595 *CHRNE* CMS is required. Further functional work is also required to ascertain the
596 importance of other potential modifiers identified in this study.
597 Our work represents a thorough study of a narrow population showing a differential
598 accumulation of damaging mutations in patients with CMS who have varying phenotypic
599 severities, building on the initial impact of *CHRNE* mutations on the NMJ. It is important to
600 remark that CMS is of particular interest among rare diseases, since drugs that influence
601 neuromuscular transmission can produce clear improvements in the affected patients (Engel
602 2007). In this sense, identifying meaningful molecular relationships between gene variants
603 allow us to gain insight into the disease mechanisms through a multiplex biomedical
604 framework, paving the way for a whole new set of computational approximations for rare
605 disease research.

606 **Acknowledgments**

607 The authors acknowledge the donors and families, Daniel Rico (Newcastle University) for his
608 contribution in early stages of the project, Anaïs Baudot (Aix Marseille Université and
609 Barcelona Supercomputing Center) for her careful revision of the manuscript, Miguel
610 Vázquez (Barcelona Supercomputing Center) for advising about Rbbt analysis, Jon Sánchez-
611 Valle (Barcelona Supercomputing Center) and Núria Olvera (Barcelona Supercomputing
612 Center and IDIBAPS) for the insightful discussions.

613 **Funding**

614 The NeurOmics and RD-Connect projects have been funded by the European Union's
615 Seventh Framework Programme for research, technological development and demonstration
616 under grant agreements no 2012-305121 and 2012-305444. I.N.C. was supported by a grant
617 for pre-doctoral contracts for the training of doctors (Project ID: SEV-2015-0493-18-2)
618 (Grant ID: PRE2018-083662) from the Spanish Ministry for Science, Innovation and
619 Universities. E.O. was supported by an AFM-Téléthon postdoctoral fellowship for the
620 duration of this work. H.L. receives support from the Canadian Institutes of Health Research
621 (Foundation Grant FDN-167281), the Canadian Institutes of Health Research and Muscular
622 Dystrophy Canada (Network Catalyst Grant for NMD4C), the Canada Foundation for
623 Innovation (CFI-JELF 38412), and the Canada Research Chairs program (Canada Research
624 Chair in Neuromuscular Genomics and Health, 950-232279). V.G. was a research fellow of
625 the Alexander von Humboldt Foundation. D.C. was supported by the European Commission's
626 Horizon 2020 Program, H2020-SC1-DTH-2018- 1, "iPC - individualizedPaediatricCure"
627 (ref. 826121).

628 **Author contributions**

629 T.C., I.T. and V.G. collected and processed the biopsies; H.L. and R.T. coordinated data
630 sharing; A.T., P.A.C.T., S.B. and S.C. coordinated and performed the omics data analysis
631 with Y.A., S.L., M.R. and M.B.; E.O. performed the experiments in zebrafish; D.C. and A.V.
632 coordinated the multilayer network analysis performed by I.N.C. All authors contributed to
633 the writing and revising of the manuscript.

634 **Ethics approval**

635 This study was approved by the Ethics committee of Sofia Medical University (protocol
636 4/15-April-2013).

637 **Competing Interest**

638 None declared.

639 **Methods**

640 ***WGS and RNA-seq***

641 Whole genome sequencing (WGS) data have been obtained from blood using the Illumina
642 TruSeq PCR-free library preparation kit. Sample sequencing was performed with the HiSeqX
643 sequencing platform (HiSeqX v1 or v2 SBS kit, 2x150 cycles), with an average mean depth
644 coverage $\geq 30X$. Samples have been analyzed using the RD-Connect specific pipeline: BWA-
645 mem for alignment; Picard for duplicate marking and GATK 3.6.0 for variant calling. RNA
646 sequencing (RNA-seq) data have been obtained from fibroblasts, using Illumina TruSeq RNA
647 Library Preparation Kit v2, sequencing with an average of 60M reads per sample (paired-end
648 2X125 cycles). Data has been processed with the following pipeline (Laurie et al. 2016):
649 STAR 2.35a for alignment, RSEM 1.3.0 for quantification, and GATK 3.6.0 for variant
650 calling. All analyses have been performed using the human genome GRCh37d5 as reference.

651 ***Copy number variants***

652 Copy Number Variants (CNVs) have been extracted using ClinCNV
653 (<https://github.com/imgag/ClinCNV>) by employing a set of Eastern European samples as a
654 background control group. Out of the 569 autosomal CNVs we selected as potential
655 candidates the CNVs of the following types that overlapped with protein-coding genes: 1)
656 whole gene gains or losses, and 2) partial losses (deletions overlapping with exons but not
657 with the whole gene). The list of potential candidates included 55 CNVs that created a total
658 of 82 whole gene gains or losses and 28 partial losses.

659 ***Compound heterozygous variants***

660 Compound heterozygous variants have been obtained by phasing the WGS variant calls with
661 the RNA-seq aligned BAM files using phASER (Castel et al. 2016). At first, variants are
662 imputed using Sanger Imputation Service with EAGLE2 pre-phasing step (Durbin 2014).
663 PhASER is then applied to extend phased regions to gene-wide haplotypes. By accurately
664 reflecting the muscle transcriptome, fibroblasts have been previously proved to be excellent
665 and minimally invasive diagnostic tools for rare neuromuscular diseases (Gonorazky et al.
666 2019). We then annotated variants with eDiVA tool (www.ediva.crg.es) (Bosio et al. 2019),
667 and removed all mutations with Genome Aggregation Database (gnomAD) (Lek et al. 2016)
668 that show allele frequency $> 3\%$ globally, all variants outside exonic and splicing regions
669 using Ensembl annotation, all synonymous mutations, and all variants with read depth
670 (coverage) smaller than 8. Afterwards we selected all genes with at least two hits on different
671 alleles as genes affected by damaging compound heterozygous variants. Each sample has
672 been processed individually throughout the whole process.

674 ***Monolayer community detection***

675 We performed a network community detection analysis using the Louvain clustering
676 algorithm (Blondel et al. 2008) implemented in R package igraph (<https://igraph.org/>) with
677 default parameters. We carried out the analysis using three (monolayer) networks, obtained

678 from Reactome database (Fabregat et al. 2018), from the Recon3D Virtual Metabolic Human
679 database (Brunk et al. 2018) (both downloaded in May 2018), and from the Integrated
680 Interaction Database (IID) (Kotlyar et al. 2016) (downloaded in October 2018). The first
681 network consists of 10,618 nodes (genes) and 875,436 edges, representing shared pathways
682 between genes. The second network consists of 1,863 nodes (genes) and 902,188 edges,
683 representing shared reaction metabolites between genes. The third network consists of 18,018
684 nodes (genes) and 947,606 edges, representing aggregated protein-protein interactions from
685 all tissues. All gene identifiers of each network were converted to NCBI Entrez gene
686 identifiers using R packages AnnotationDbi v1.44.0 and org.Hs.eg.db v3.7.0
687 (<http://bioconductor.org/>). After detecting the community structure from each layer
688 independently, we retrieved the community membership of the genes of interest, henceforth
689 called “CMS linked genes”, i.e. known CMS causal genes, and severe and not-severe
690 compound heterozygous variants and CNVs. We then defined a community similarity
691 measure as Jaccard Index, i.e. the number of shared genes of interest between the
692 communities divided by the sum of the total number of genes of each community.

693 ***Multilayer community detection***

694 We constructed a multilayer gene network composed of the three monolayer networks
695 described in the previous section (Reactome, Virtual Metabolic Human and Integrated
696 Interaction Database). Each of these three networks represents one layer of the multilayer
697 network and, in general, three facets of fundamental molecular processes in the cell (**Suppl.**
698 **Figure 11**). The multilayer community detection analysis was performed by using MolTi
699 software (Didier, Brun, and Baudot 2015), which adapts the Louvain clustering algorithm
700 with modularity maximization to multilayer networks. The algorithm is parametrized by the
701 resolution (γ): the higher the value of γ , the smaller the size of the detected multilayer
702 communities. By varying the resolution parameter γ it is possible to uncover the modular
703 structure of network communities (Fortunato and Barthelemy 2007). By exploring a wide
704 range of resolution parameter values, we identified $\gamma=4$ (727 communities, each one
705 composed of 26.46 genes on average) as an extreme value before both size and number of the
706 detected multilayer communities stabilize (**Suppl. Figure 12**). The most dramatic changes in
707 number and composition of detected communities are observed in the resolution parameter
708 interval $\gamma \in (0,4]$. We, therefore, used this parameter interval to test the hypothesis that
709 disease-related genes consistently appear in the same multilayer communities, as well as to
710 identify modules containing CMS linked genes within them. In this analysis, we define a
711 module as a group of CMS linked genes that are systematically found to be part of the same
712 multilayer community while increasing the resolution parameter (see Supplementary
713 Information "Multilayer community detection analysis").

714 ***Additional analyses and code availability***

715 We retrieved known CMS causal genes from the GeneTable of Neuromuscular Disorders
716 (<http://www.musclegenetable.fr>, version November 2018) (Bonne, Rivier, and Hamroun
717 2017). Segregation analysis of WGS data has been performed using Rbbt (Vázquez et al.

718 2010). DisGeNET database (Piñero et al. 2017) was downloaded in November 2018. The
719 association between CMS severity, demographic factors and clinical tests was assessed with a
720 two-tailed Fisher's test using R statistical environment (www.R-project.org). Networks were
721 rendered with Cytoscape (Saito et al. 2012). We used VCFtools (Danecek et al. 2011) to
722 compute familial relatedness Ω among patients, scaled to $-\log_2(2\Omega)$. We used Enrichr (E. Y.
723 Chen et al. 2013) for the functional enrichment analysis of the gene lists under study. We
724 used Ensembl Variant Effect Predictor (VEP) (McLaren et al. 2016) to assess the impact of
725 the compound heterozygous variants in the genes of the severe-specific largest module.
726 Expression levels in tissues of interest (GTEx and Illumina Body Map) were retrieved from
727 EBI Expression Atlas (www.ebi.ac.uk/) by filtering with the following keywords: 'nerve',
728 'muscle cell', 'fibroblast' and 'nervous system' (0.5 TPM default cutoff). We used
729 Expression Atlas expression level categories: low (0.5 to 10 TPM), medium (11 to 1000
730 TPM), and high (more than 1000 TPM) (Petryszak et al. 2016). Synaptic localization was
731 retrieved from the UniProt database (<https://www.uniprot.org/>). All code from the original
732 analysis is available for reproducibility purposes at: <https://github.com/ikernunezca/CMS>.
733 The analysis of multilayer community communities can also be performed using CmmD
734 (Nuñez-Carpintero et al., 2021) (<https://github.com/ikernunezca/CmmD>) with parameters:
735 resolution_start: 0, resolution_end: 4, interval: 0.5 and the CMS linked genes as nodelist.

736 ***Zebrafish morpholino injections***

737 Zebrafish have one orthologue of human *USH2a*: *ush2a*, as identified using the UCSC
738 database (<http://genome.ucsc.edu/>, GRCz11/danRer11 assembly). We confirmed that *ush2a* is
739 expressed throughout the first 5 days post fertilization (dpf). Gene Tools LLC (USA) then
740 designed and synthesized an antisense morpholino oligonucleotide (MO) targeting the splice
741 donor site of exon 3/intron 3 of *ush2a* (5'-3' GAGAAATGCTGCTCACCTGTAGAGC,
742 ENSDART00000086201.5). We also obtained a control MO that targets a human beta-globin
743 mutation (5'-3' CCTCTTACCTCAGTTACAATTTATA). MOs were diluted to 2 ng/nl in
744 Danieau buffer (58 mM NaCl, 5 mM HEPES, 0.7 mM KCl, 0.6 mM Ca(NO₃)₂, 0.4 mM
745 MgSO₄; pH 7.6) and supplemented with 1% phenol red, before being injected into the yolk-
746 sac of 1-cell stage embryos. A range of doses between 6 and 18 ng per 1-cell stage embryo
747 were trialed for success in reducing *ush2a* expression and producing a measurable phenotypic
748 change. A dose of 18 ng per 1-cell stage embryo was selected for behavioral and
749 morphological analysis, as survival was not significantly affected for any dose tested.
750 Embryos were maintained at 28.5°C in blue water (system water with 0.1 µg/ml Methylene
751 Blue) for up to 5 dpf and survival recorded daily. At 2 dpf zebrafish were imaged using a
752 Leica EZ4 W stereomicroscope and eye size and length measured using Fiji (ImageJ).

753 ***Chorion movement analysis in zebrafish***

754 At 1 dpf (24 hours post fertilization), zebrafish were recorded in their chorions for 1 minute
755 at 30 frames per second using a Leica EZ4 W stereomicroscope. Videos were analyzed using
756 DanioScope software (Noldus Information Technology Inc., Leesburg, VA) to automatically
757 assess duration of bursts and burst count/minute (bursts are full rotations performed by the

758 zebrafish within the chorion).

759 ***Touch response analysis***

760 At 2 dpf, a touch response assay was performed as previously described (O'Connor et al.
761 2018). Only fish with a normal phenotype were used for movement analysis. Briefly, fish that
762 had not hatched from the chorion were enzymatically dechorionated with pronase (1 mg/ml,
763 Sigma) for 10 min in blue water, followed by 3x washes in blue water. An individual fish was
764 placed in a petri dish containing blue water and a Sony RX0 II (DSC-RX0M2) camera was
765 placed 20 cm above the petri dish. A ruler with 1 mm markings was used as a scale for
766 recordings. A gel loading pipette tip was used to touch the zebrafish on the back of the head
767 and the response recorded. Videos were imported into Fiji ImageJ (Schindelin et al. 2012) as
768 Ffmpeg movies and movements analyzed using the Trackmate plugin (Tinevez et al. 2017).
769 Values for average speed were exported and used to derive initial acceleration.

770 ***RNA isolation, cDNA synthesis and RT-PCR in zebrafish***

771 RNA was isolated from pools of around 20 2 dpf zebrafish (control MO and *ush2a* MO-
772 injected) following removal of chorions with pronase (*Streptomyces griseus*, Roche, 1 mg/ml
773 in blue water). Zebrafish were washed 3 times with blue water, euthanized with a 1:1 ratio of
774 fresh system water:4 mg/ml tricaine methanesulfonate (Sigma). Fish were homogenized in
775 RLT buffer (RNeasy mini kit, Qiagen) using 5 mm stainless steel beads with a TissueLyser II
776 (Qiagen) at 25 Hz for 2 mins. RNA was then isolated following the RNeasy kit
777 manufacturer's instructions, including on-column DNase digestion. RNA was measured
778 using a Nanodrop ND-1000 and 1 µg used for cDNA synthesis according to manufacturer's
779 instructions (5X All-In-One RT MasterMix, abm). Reverse-transcriptase PCR (RT-PCR) was
780 performed to check for *ush2a* gene expression and knockdown success in MO-treated
781 embryos, using MyTaq™ DNA Polymerase (Meridian Bioscience) and primers as follows:
782 *eef1a11l1* forward 5'-CTGGAGGCCAGCTCAAACATGG-3', reverse 5'-
783 CTTGCTGTCTCCAGCCACATTAC-3' and *ush2a* forward 5'-
784 CTGGGCACACTTGGCTCTAC -3', reverse 5'-TTCTTCAATCTCCCTGTTGGTT-3'.

785 ***Immunofluorescent staining, imaging and analysis of zebrafish neuromuscular junctions*** 786 ***and muscle fibers***

787 Whole mount staining of 2 dpf zebrafish NMJs was performed as previously described
788 (O'Connor et al. 2019). Briefly, a mouse anti-synaptic vesicle protein 2 (SV2) antibody was
789 used to visualize motor neurons (1:200, AB2315387, Developmental Studies Hybridoma
790 Bank) and Alexa Fluor 488- α -bungarotoxin conjugate (1:1000, B13422, Invitrogen) was used
791 for visualizing acetylcholine receptors (AChRs). Phalloidin-iFluor 594 was used to visualize
792 filamentous actin within muscle fibers (1:1000, ab176757). Z-stack images encompassing the
793 depth of the midsection of the zebrafish tail were obtained using a 20 \times air objective on an
794 LSM800 confocal microscope. Analysis of NMJ structure was performed as previously
795 described (O'Connor et al. 2019), using Fiji (ImageJ, Madison, WI, USA). The number of
796 SV2-positive and α -bungarotoxin-positive clusters per 100 μm^2 were measured. Co-
797 localization analysis between SV2 and α -bungarotoxin was performed on maximum intensity

798 projections using the ‘JACoP’ Fiji plugin (Bolte & Cordelières, 2006). Briefly, each
799 fluorophore was subject to manual thresholding to remove background, and the Mander’s
800 correlation coefficient calculated to give a value between 0 and 1, reflecting the degree of co-
801 occurrence of signals between both SV2 and α -bungarotoxin, and α -bungarotoxin with SV2.
802 For phalloidin-stained fish, average myotome size was measured, and degree of fiber
803 dispersion quantified using the directionality plugin. Data was collected from at least 4
804 myotomes per fish.

805 ***Statistics for zebrafish experiments***

806 Statistical analysis was performed using GraphPad Prism software (v9.3.0). Outliers were
807 removed from data using the ROUT method (Q = 1 %). Cleaned data was tested for normal
808 distribution then depending on outcome either a nonparametric Mann-Whitney test or
809 parametric unpaired t-test were applied for behavioral studies and degree of dispersion. For
810 NMJ morphology experiments in which 4+ myotomes (technical replicates) per fish
811 (biological replicates) were analyzed, data was assessed for significance using a nested t-test
812 to avoid pseudoreplication. Statistical significance was taken as $p < 0.05$, degrees of freedom
813 (df) and t-value are given for all parametric tests, and n numbers listed in the results section.
814 Survival analysis was performed using the log-rank test comparing WT to each other
815 condition, and threshold for significance was corrected for multiple comparisons using the
816 Bonferroni method ($p < 0.006$). Zebrafish studies were blinded before image/video
817 acquisition and unblinded following analysis.

818 References

- 819 Abicht, A., R. Stucka, V. Karcagi, A. Herczegfalvi, R. Horváth, W. Mortier, U. Schara, et al.
820 1999. "A Common Mutation (Epsilon1267delG) in Congenital Myasthenic Patients of
821 Gypsy Ethnic Origin." *Neurology* 53 (7): 1564–69.
822 <https://doi.org/10.1212/wnl.53.7.1564>.
- 823 Abicht, Angela, Juliane Müller, and Hanns Lochmüller. 1993. "Congenital Myasthenic
824 Syndromes." In *GeneReviews®*, edited by Margaret P. Adam, Holly H. Arding, and
825 Roberta A. Pagon, Stephanie E. Wallace, Lora JH Bean, Karen Stephens, and Anne
826 Amemiya. Seattle (WA): University of Washington, Seattle.
827 <http://www.ncbi.nlm.nih.gov/books/NBK1168/>.
- 828 Amin, Mutaz, Yousuf Bakhit, Mahmoud Koko, Mohamed Osama Mirgahni Ibrahim, M. A.
829 Salih, Muntaser Ibrahim, and Osheik A. Seidi. 2019. "Rare Variant in LAMA2 Gene
830 Causing Congenital Muscular Dystrophy in a Sudanese Family. A Case Report." *Acta*
831 *Myologica: Myopathies and Cardiomyopathies: Official Journal of the*
832 *Mediterranean Society of Myology* 38 (1): 21–24.
- 833 Andreose, J. S., C. Sala, and G. Fumagalli. 1994. "Immunolocalization of Chromogranin B,
834 Secretogranin II, Calcitonin Gene-Related Peptide and Substance P at Developing and
835 Adult Neuromuscular Synapses." *Neuroscience Letters* 174 (2): 177–80.
- 836 Arikawa-Hirasawa, Eri, William R. Wilcox, Alexander H. Le, Neil Silverman, Prasanthi
837 Govindraj, John R. Hassell, and Yoshihiko Yamada. "Dyssegmental Dysplasia,
838 Silverman-Handmaker Type, Is Caused by Functional Null Mutations of the Perlecan
839 Gene." *Nature Genetics* 27, no. 4 (April 2001): 431–34.
840 <https://doi.org/10.1038/86941>.
- 841 Arikawa-Hirasawa, Eri, Alexander H. Le, Ichizo Nishino, Ikuya Nonaka, Nicola C. Ho, Clair
842 A. Francomano, Prasanthi Govindraj, et al. 2002. "Structural and Functional
843 Mutations of the Perlecan Gene Cause Schwartz-Jampel Syndrome, with Myotonic
844 Myopathy and Chondrodysplasia." *American Journal of Human Genetics* 70 (5):
845 1368–75. <https://doi.org/10.1086/340390>.
- 846 Astigarraga, Sergio, Kerstin Hofmeyer, Reza Farajian, and Jessica E. Treisman. 2010. "Three
847 Drosophila Liprins Interact to Control Synapse Formation." *The Journal of*
848 *Neuroscience: The Official Journal of the Society for Neuroscience* 30 (46): 15358–
849 68. <https://doi.org/10.1523/JNEUROSCI.1862-10.2010>.
- 850 Austin-Tse, Christina A., Diana L. Mandelker, Andrea M. Oza, Heather Mason-Suares, Heidi
851 L. Rehm, and Sami S. Amr. 2018. "Analysis of Intragenic USH2A Copy Number
852 Variation Unveils Broad Spectrum of Unique and Recurrent Variants." *European*
853 *Journal of Medical Genetics* 61 (10): 621–26.
854 <https://doi.org/10.1016/j.ejmg.2018.04.006>.
- 855 Barik, Arnab, Yisheng Lu, Anupama Sathyamurthy, Andrew Bowman, Chengyong Shen, Lei
856 Li, Wen-cheng Xiong, and Lin Mei. 2014. "LRP4 Is Critical for Neuromuscular
857 Junction Maintenance." *The Journal of Neuroscience: The Official Journal of the*
858 *Society for Neuroscience* 34 (42): 13892–905.

- 859 <https://doi.org/10.1523/JNEUROSCI.1733-14.2014>.
- 860 Beeson, David. 2016. "Congenital Myasthenic Syndromes: Recent Advances." *Current*
861 *Opinion in Neurology* 29 (5): 565–71.
862 <https://doi.org/10.1097/WCO.0000000000000370>.
- 863 Bernadzki, Krzysztof M., Marta Gawor, Marcin Pęziński, Paula Mazurek, Paweł
864 Niewiadomski, Maria J. Rędownicz, and Tomasz J. Prószyński. 2017. "Liprin- α -1 Is a
865 Novel Component of the Murine Neuromuscular Junction and Is Involved in the
866 Organization of the Postsynaptic Machinery." *Scientific Reports* 7 (1): 9116.
867 <https://doi.org/10.1038/s41598-017-09590-7>.
- 868 Bertini, Enrico, Adele D'Amico, Francesca Gualandi, and Stefania Petrini. 2011. "Congenital
869 Muscular Dystrophies: A Brief Review." *Seminars in Pediatric Neurology* 18 (4):
870 277–88. <https://doi.org/10.1016/j.spen.2011.10.010>.
- 871 Bevilacqua, Jorge A., Marian Lara, Jorge Díaz, Mario Campero, Jessica Vázquez, and
872 Ricardo A. Maselli. 2017. "Congenital Myasthenic Syndrome Due to DOK7
873 Mutations in a Family from Chile." *European Journal of Translational Myology* 27
874 (3): 6832. <https://doi.org/10.4081/ejtm.2017.6832>.
- 875 Blondel, Vincent D., Jean-Loup Guillaume, Renaud Lambiotte, and Etienne Lefebvre. 2008.
876 "Fast Unfolding of Communities in Large Networks." *Journal of Statistical*
877 *Mechanics: Theory and Experiment* 2008 (10): P10008.
878 <https://doi.org/10.1088/17425468/2008/10/P10008>.
- 879 Bolte, Sussane, and Fabrice P. Cordelières. "A Guided Tour into Subcellular Colocalization
880 Analysis in Light Microscopy." *Journal of Microscopy* 224, no. 3 (2006): 213–32.
881 <https://doi.org/10.1111/j.1365-2818.2006.01706.x>.
- 882 Bonne, Gisèle, François Rivier, and Dalil Hamroun. 2017. "The 2018 Version of the Gene
883 Table of Monogenic Neuromuscular Disorders (Nuclear Genome)." *Neuromuscular*
884 *Disorders: NMD* 27 (12): 1152–83. <https://doi.org/10.1016/j.nmd.2017.10.005>.
- 885 Bönnemann, Carsten G., Ching H. Wang, Susana Quijano-Roy, Nicolas Deconinck, Enrico
886 Bertini, Ana Ferreiro, Francesco Muntoni, et al. 2014. "Diagnostic Approach to the
887 Congenital Muscular Dystrophies." *Neuromuscular Disorders: NMD* 24 (4): 289–
888 311. <https://doi.org/10.1016/j.nmd.2013.12.011>.
- 889 Bork, P., and R. F. Doolittle. 1992. "Proposed Acquisition of an Animal Protein Domain by
890 Bacteria." *Proceedings of the National Academy of Sciences of the United States of*
891 *America* 89 (19): 8990–94.
- 892 Bosio, Mattia, Oliver Drechsel, Rubayte Rahman, Francesc Muyas, Raquel Rabionet, Daniela
893 Bezdán, Laura Domenech Salgado, et al. 2019. "EDiVA-Classification and
894 Prioritization of Pathogenic Variants for Clinical Diagnostics." *Human Mutation*,
895 April. <https://doi.org/10.1002/humu.23772>.
- 896 Boycott, Kym M., Megan R. Vanstone, Dennis E. Bulman, and Alex E. MacKenzie. 2013.
897 "Rare-Disease Genetics in the Era of next-Generation Sequencing: Discovery to
898 Translation." *Nature Reviews Genetics* 14 (10): 681–91.
899 <https://doi.org/10.1038/nrg3555>.
- 900 Brunk, Elizabeth, Swagatika Sahoo, Daniel C. Zielinski, Ali Altunkaya, Andreas Dräger,

- 901 Nathan Mih, Francesco Gatto, et al. 2018. “Recon3D Enables a Three-Dimensional
902 View of Gene Variation in Human Metabolism.” *Nature Biotechnology* 36 (3): 272–
903 81. <https://doi.org/10.1038/nbt.4072>.
- 904 Buphamalai, Pisanu, Tomislav Kokotovic, Vanja Nagy, and Jörg Menche. 2021. ‘Network
905 Analysis Reveals Rare Disease Signatures across Multiple Levels of Biological
906 Organization’. *Nature Communications* 12 (1): 6306. [https://doi.org/10.1038/s41467-
907 021-26674-1](https://doi.org/10.1038/s41467-021-26674-1).
- 908 Cantini, Laura, Enzo Medico, Santo Fortunato, and Michele Caselle. 2015. “Detection of
909 Gene Communities in Multi-Networks Reveals Cancer Drivers.” *Scientific Reports* 5
910 (December): 17386. <https://doi.org/10.1038/srep17386>.
- 911 Castel, Stephane E., Pejman Mohammadi, Wendy K. Chung, Yufeng Shen, and Tuuli
912 Lappalainen. 2016. “Rare Variant Phasing and Haplotypic Expression from RNA
913 Sequencing with PhASER.” *Nature Communications* 7: 12817.
914 <https://doi.org/10.1038/ncomms12817>.
- 915 Castro-Giner, Francesc, Peter Ratcliffe, and Ian Tomlinson. 2015. “The Mini-Driver Model
916 of Polygenic Cancer Evolution.” *Nature Reviews. Cancer* 15 (11): 680–85.
917 <https://doi.org/10.1038/nrc3999>.
- 918 Chen, Edward Y., Christopher M. Tan, Yan Kou, Qiaonan Duan, Zichen Wang, Gabriela Vaz
919 Meirelles, Neil R. Clark, and Avi Ma’ayan. 2013. “Enrichr: Interactive and
920 Collaborative HTML5 Gene List Enrichment Analysis Tool.” *BMC Bioinformatics* 14
921 (April): 128. <https://doi.org/10.1186/1471-2105-14-128>.
- 922 Chen, Yuewen, Jinying Xu, Xiaopu Zhou, Saijuan Liu, Yulin Zhang, Shuangshuang Ma,
923 Amy K. Y. Fu, Nancy Y. Ip, and Yu Chen. 2019. “Changes of Protein
924 Phosphorylation Are Associated with Synaptic Functions during the Early Stage of
925 Alzheimer’s Disease.” *ACS Chemical Neuroscience* 10 (9): 3986–96.
926 <https://doi.org/10.1021/acscemneuro.9b00190>.
- 927 Clausen, Lisa, Judith Cossins, and David Beeson. 2018. “Beta-2 Adrenergic Receptor
928 Agonists Enhance AChR Clustering in C2C12 Myotubes: Implications for Therapy of
929 Myasthenic Disorders.” *Journal of Neuromuscular Diseases* 5 (2): 231–40.
930 <https://doi.org/10.3233/JND-170293>.
- 931 Dagur, Pradeep K., and J. Philip McCoy. 2015. “Endothelial-Binding, Proinflammatory T
932 Cells Identified by MCAM (CD146) Expression: Characterization and Role in Human
933 Autoimmune Diseases.” *Autoimmunity Reviews* 14 (5): 415–22.
934 <https://doi.org/10.1016/j.autrev.2015.01.003>.
- 935 Danecek, P., A. Auton, G. Abecasis, C. A. Albers, E. Banks, M. A. DePristo, R. E.
936 Handsaker, et al. 2011. “The Variant Call Format and VCFtools.” *Bioinformatics* 27
937 (15): 2156–58. <https://doi.org/10.1093/bioinformatics/btr330>.
- 938 Didier, Gilles, Christine Brun, and Anaïs Baudot. 2015. “Identifying Communities from
939 Multiplex Biological Networks.” *PeerJ* 3: e1525. <https://doi.org/10.7717/peerj.1525>.
- 940 Dimova, Ivanka, and Ivo Kremensky. 2018. “LAMA2 Congenital Muscle Dystrophy: A
941 Novel Pathogenic Mutation in Bulgarian Patient.” *Case Reports in Genetics* 2018:
942 3028145. <https://doi.org/10.1155/2018/3028145>.

- 943 Downes, Gerald B., and Michael Granato. 2006. "Supraspinal Input Is Dispensable to
944 Generate Glycine-Mediated Locomotive Behaviors in the Zebrafish Embryo."
945 *Journal of Neurobiology* 66, no. 5: 437–51. <https://doi.org/10.1002/neu.20226>.
- 946 Durbin, Richard. 2014. "Efficient Haplotype Matching and Storage Using the Positional
947 Burrows-Wheeler Transform (PBWT)." *Bioinformatics (Oxford, England)* 30 (9):
948 1266–72. <https://doi.org/10.1093/bioinformatics/btu014>.
- 949 Eklund, L., J. Pihola, J. Komulainen, R. Sormunen, C. Ongvarrasopone, R. Fässler, A.
950 Muona, et al. 2001. "Lack of Type XV Collagen Causes a Skeletal Myopathy and
951 Cardiovascular Defects in Mice." *Proceedings of the National Academy of Sciences of
952 the United States of America* 98 (3): 1194–99.
953 <https://doi.org/10.1073/pnas.031444798>.
- 954 Engel, Andrew G. 2007. "The Therapy of Congenital Myasthenic Syndromes."
955 *Neurotherapeutics: The Journal of the American Society for Experimental
956 NeuroTherapeutics* 4 (2): 252–57. <https://doi.org/10.1016/j.nurt.2007.01.001>.
- 957 Engel, Andrew G., Xin-Ming Shen, Duygu Selcen, and Steven M. Sine. 2015. "Congenital
958 Myasthenic Syndromes: Pathogenesis, Diagnosis, and Treatment." *The Lancet.
959 Neurology* 14 (4): 420–34. [https://doi.org/10.1016/S1474-4422\(14\)70201-7](https://doi.org/10.1016/S1474-4422(14)70201-7).
- 960 Estephan, Eduardo de Paula, Antonio Alberto Zambon, Paulo Eurípedes Marchiori, André
961 Macedo Serafim da Silva, Vitor Marques Caldas, Cristiane Araújo Martins Moreno,
962 Umbertina Conti Reed, et al. 2018. "Clinical Variability of Early-Onset Congenital
963 Myasthenic Syndrome Due to Biallelic RAPSN Mutations in Brazil." *Neuromuscular
964 Disorders* 28 (11): 961–64. <https://doi.org/10.1016/j.nmd.2018.08.007>.
- 965 Fabregat, Antonio, Steven Jupe, Lisa Matthews, Konstantinos Sidiropoulos, Marc Gillespie,
966 Phani Garapati, Robin Haw, et al. 2018. "The Reactome Pathway Knowledgebase."
967 *Nucleic Acids Research* 46 (D1): D649–55. <https://doi.org/10.1093/nar/gkx1132>.
- 968 Fareed, Mohd, and Mohammad Afzal. 2017. "Genetics of Consanguinity and Inbreeding in
969 Health and Disease." *Annals of Human Biology* 44 (2): 99–107.
970 <https://doi.org/10.1080/03014460.2016.1265148>.
- 971 Finsterer, Josef. 2019. "Congenital Myasthenic Syndromes." *Orphanet Journal of Rare
972 Diseases* 14 (1): 57. <https://doi.org/10.1186/s13023-019-1025-5>.
- 973 Forrest, Katharine, Jemima E. Mellerio, Stephanie Robb, Patricia J. C. Dopping-Hepenstal,
974 John A. McGrath, Lu Liu, Stefan J. A. Buk, Safa Al-Sarraj, Elizabeth Wraige, and
975 Heinz Jungbluth. 2010. "Congenital Muscular Dystrophy, Myasthenic Symptoms and
976 Epidermolysis Bullosa Simplex (EBS) Associated with Mutations in the PLEC1 Gene
977 Encoding Plectin." *Neuromuscular Disorders: NMD* 20 (11): 709–11.
978 <https://doi.org/10.1016/j.nmd.2010.06.003>.
- 979 Fortunato, S., and M. Barthelemy. 2007. "Resolution Limit in Community Detection."
980 *Proceedings of the National Academy of Sciences* 104 (1): 36–41.
981 <https://doi.org/10.1073/pnas.0605965104>.
- 982 Garg, Divyani, and Vinay Goyal. "Positive Response to Inhaled Salbutamol in Congenital
983 Myasthenic Syndrome Due to CHRNE Mutation." *Muscle & Nerve* n/a, no. n/a.
984 Accessed June 2, 2022. <https://doi.org/10.1002/mus.27563>.

- 985 Goh, K.-I., M. E. Cusick, D. Valle, B. Childs, M. Vidal, and A.-L. Barabasi. 2007. “The
986 Human Disease Network.” *Proceedings of the National Academy of Sciences* 104
987 (21): 8685–90. <https://doi.org/10.1073/pnas.0701361104>.
- 988 Gonorazky, Hernan D., Sergey Naumenko, Arun K. Ramani, Viswateja Nelakuditi, Pouria
989 Mashouri, Peiqui Wang, Dennis Kao, et al. 2019. “Expanding the Boundaries of RNA
990 Sequencing as a Diagnostic Tool for Rare Mendelian Disease.” *American Journal of*
991 *Human Genetics* 104 (3): 466–83. <https://doi.org/10.1016/j.ajhg.2019.01.012>.
- 992 Gosak, Marko, Rene Markovič, Jurij Dolenšek, Marjan Slak Rupnik, Marko Marhl, Andraž
993 Stožer, and Matjaž Perc. 2018. “Network Science of Biological Systems at Different
994 Scales: A Review.” *Physics of Life Reviews* 24: 118–35.
995 <https://doi.org/10.1016/j.plrev.2017.11.003>.
- 996 Gowen, B. B., T. K. Borg, A. Ghaffar, and E. P. Mayer. 2000. “Selective Adhesion of
997 Macrophages to Denatured Forms of Type I Collagen Is Mediated by Scavenger
998 Receptors.” *Matrix Biology: Journal of the International Society for Matrix Biology*
999 19 (1): 61–71.
- 1000 Grevengoed, Trisha J., Eric L. Klett, and Rosalind A. Coleman. 2014. “Acyl-CoA
1001 Metabolism and Partitioning.” *Annual Review of Nutrition* 34: 1–30.
1002 <https://doi.org/10.1146/annurev-nutr-071813-105541>.
- 1003 Guillon, Emilie, Sandrine Bretaud, and Florence Ruggiero. 2016. “Slow Muscle Precursors
1004 Lay Down a Collagen XV Matrix Fingerprint to Guide Motor Axon Navigation.” *The*
1005 *Journal of Neuroscience: The Official Journal of the Society for Neuroscience* 36 (9):
1006 2663–76. <https://doi.org/10.1523/JNEUROSCI.2847-15.2016>.
- 1007 Halu, Arda, Manlio De Domenico, Alex Arenas, and Amitabh Sharma. 2017. “The Multiplex
1008 Network of Human Diseases.” *BioRxiv*. <https://doi.org/10.1101/100370>.
- 1009 Han, Shanshan, Xiliang Liu, Shanglun Xie, Meng Gao, Fei Liu, Shanshan Yu, Peng Sun, et
1010 al. 2018. “Knockout of Ush2a Gene in Zebrafish Causes Hearing Impairment and
1011 Late Onset Rod-Cone Dystrophy.” *Human Genetics* 137, no. 10: 779–94.
1012 <https://doi.org/10.1007/s00439-018-1936-6>.
- 1013 Hull, Sarah, Gavin Arno, Anthony G. Robson, Suzanne Broadgate, Vincent Plagnol, Martin
1014 McKibbin, Stephanie Halford, et al. 2016. “Characterization of CDH3-Related
1015 Congenital Hypotrichosis With Juvenile Macular Dystrophy.” *JAMA Ophthalmology*
1016 134 (9): 992–1000. <https://doi.org/10.1001/jamaophthalmol.2016.2089>.
- 1017 Huzé, Caroline, Stéphanie Bauché, Pascale Richard, Frédéric Chevessier, Evelyne Goillot,
1018 Karen Gaudon, Asma Ben Ammar, et al. 2009. “Identification of an Agrin Mutation
1019 That Causes Congenital Myasthenia and Affects Synapse Function.” *American*
1020 *Journal of Human Genetics* 85 (2): 155–67.
1021 <https://doi.org/10.1016/j.ajhg.2009.06.015>.
- 1022 Iozzo, Renato V., and Liliana Schaefer. 2015. “Proteoglycan Form and Function: A
1023 Comprehensive Nomenclature of Proteoglycans.” *Matrix Biology: Journal of the*
1024 *International Society for Matrix Biology* 42 (March): 11–55.
1025 <https://doi.org/10.1016/j.matbio.2015.02.003>.
- 1026 Ito, Mikako, and Kinji Ohno. 2018. “Protein-Anchoring Therapy to Target Extracellular

- 1027 Matrix Proteins to Their Physiological Destinations.” *Matrix Biology: Journal of the*
1028 *International Society for Matrix Biology* 68–69: 628–36.
1029 <https://doi.org/10.1016/j.matbio.2018.02.014>.
- 1030 Johansson, Malin E. V., Kristina A. Thomsson, and Gunnar C. Hansson. 2009. “Proteomic
1031 Analyses of the Two Mucus Layers of the Colon Barrier Reveal That Their Main
1032 Component, the Muc2 Mucin, Is Strongly Bound to the Fcgbp Protein.” *Journal of*
1033 *Proteome Research* 8 (7): 3549–57. <https://doi.org/10.1021/pr9002504>.
- 1034 Kaneko-Goto, Tomomi, Yuki Sato, Sayako Katada, Emi Kinameri, Sei-ichi Yoshihara,
1035 Atsushi Nishiyori, Mitsuhiro Kimura, et al. 2013. “Goofy Coordinates the Acuity of
1036 Olfactory Signaling.” *The Journal of Neuroscience: The Official Journal of the*
1037 *Society for Neuroscience* 33 (32): 12987–96, 12996a.
1038 <https://doi.org/10.1523/JNEUROSCI.4948-12.2013>.
- 1039 Karczewski, Konrad J., and Michael P. Snyder. 2018. “Integrative Omics for Health and
1040 Disease.” *Nature Reviews Genetics* 19 (5): 299–310.
1041 <https://doi.org/10.1038/nrg.2018.4>.
- 1042 Karczewski, Konrad J., Laurent C. Francioli, Grace Tiao, Beryl B. Cummings, Jessica
1043 Alföldi, Qingbo Wang, Ryan L. Collins, et al. “The Mutational Constraint Spectrum
1044 Quantified from Variation in 141,456 Humans.” *Nature* 581, no. 7809 (May 2020):
1045 434–43. <https://doi.org/10.1038/s41586-020-2308-7>.
- 1046 Keller, Kate E., Ying Ying Sun, Janice A. Vranka, Lauren Hayashi, and Ted S. Acott. 2012.
1047 “Inhibition of Hyaluronan Synthesis Reduces Versican and Fibronectin Levels in
1048 Trabecular Meshwork Cells.” *PloS One* 7 (11): e48523.
1049 <https://doi.org/10.1371/journal.pone.0048523>.
- 1050 Kirschner, Janbernd, Ingrid Hausser, Yaqun Zou, Gudrun Schreiber, Hans-Jürgen Christen,
1051 Susan C. Brown, Ingrun Anton-Lamprecht, Francesco Muntoni, Folker Hanefeld, and
1052 Carsten G. Bönnemann. 2005. “Ullrich Congenital Muscular Dystrophy: Connective
1053 Tissue Abnormalities in the Skin Support Overlap with Ehlers-Danlos Syndromes.”
1054 *American Journal of Medical Genetics. Part A* 132A (3): 296–301.
1055 <https://doi.org/10.1002/ajmg.a.30443>.
- 1056 Kivelä, Mikko, Alexandre Arenas, Marc Barthelemy, James P. Gleeson, Yamir Moreno, and
1057 Mason A. Porter. 2014. “Multilayer Networks.” *Journal of Complex Networks* 2 (3):
1058 203–71. <https://doi.org/10.1093/comnet/cnu016>.
- 1059 Kotlyar, Max, Chiara Pastrello, Nicholas Sheahan, and Igor Jurisica. 2016. “Integrated
1060 Interactions Database: Tissue-Specific View of the Human and Model Organism
1061 Interactomes.” *Nucleic Acids Research* 44 (D1): D536–541.
1062 <https://doi.org/10.1093/nar/gkv1115>.
- 1063 Kousi, M., and N. Katsanis. 2015. “Genetic Modifiers and Oligogenic Inheritance.” *Cold*
1064 *Spring Harbor Perspectives in Medicine* 5 (6): a017145–a017145.
1065 <https://doi.org/10.1101/cshperspect.a017145>.
- 1066 Kraft-Sheleg, Ortal, Shelly Zaffryar-Eilot, Olga Genin, Wesal Yaseen, Sharon Soueid-
1067 Baumgarten, Ofra Kessler, Tatyana Smolkin, et al. 2016. “Localized LoxL3-
1068 Dependent Fibronectin Oxidation Regulates Myofiber Stretch and Integrin-Mediated

- 1069 Adhesion.” *Developmental Cell* 36 (5): 550–61.
1070 <https://doi.org/10.1016/j.devcel.2016.02.009>.
- 1071 Laskowski, M., and I. Kato. 1980. “Protein Inhibitors of Proteinases.” *Annual Review of*
1072 *Biochemistry* 49: 593–626. <https://doi.org/10.1146/annurev.bi.49.070180.003113>.
- 1073 Laurie, Steve, Marcos Fernandez-Callejo, Santiago Marco-Sola, Jean-Remi Trotta, Jordi
1074 Camps, Alejandro Chacón, Antonio Espinosa, et al. 2016. “From Wet-Lab to
1075 Variations: Concordance and Speed of Bioinformatics Pipelines for Whole Genome
1076 and Whole Exome Sequencing.” *Human Mutation* 37, (12): 1263–71.
1077 <https://doi.org/10.1002/humu.23114>.
- 1078 Lee, Manon, David Beeson, and Jacqueline Palace. 2018. “Therapeutic Strategies for
1079 Congenital Myasthenic Syndromes.” *Annals of the New York Academy of Sciences*
1080 1412 (1): 129–36. <https://doi.org/10.1111/nyas.13538>.
- 1081 Lek, Monkol, Konrad J. Karczewski, Eric V. Minikel, Kaitlin E. Samocha, Eric Banks,
1082 Timothy Fennell, Anne H. O’Donnell-Luria, et al. 2016. “Analysis of Protein-Coding
1083 Genetic Variation in 60,706 Humans.” *Nature* 536 (7616): 285–91.
1084 <https://doi.org/10.1038/nature19057>.
- 1085 Li, Lei O., Trisha J. Grevengoed, David S. Paul, Olga Ilkayeva, Timothy R. Koves, Florencia
1086 Pascual, Christopher B. Newgard, Deborah M. Muoio, and Rosalind A. Coleman.
1087 2015. “Compartmentalized Acyl-CoA Metabolism in Skeletal Muscle Regulates
1088 Systemic Glucose Homeostasis.” *Diabetes* 64 (1): 23–35.
1089 <https://doi.org/10.2337/db13-1070>.
- 1090 Lochmüller, Hanns, Dorota M. Badowska, Rachel Thompson, Nine V. Knoers, Annemieke
1091 Aartsma-Rus, Ivo Gut, Libby Wood, et al. 2018. “RD-Connect, NeurOmics and
1092 EURenOmics: Collaborative European Initiative for Rare Diseases.” *European*
1093 *Journal of Human Genetics: EJHG* 26 (6): 778–85.
1094 <https://doi.org/10.1038/s41431018-0115-5>.
- 1095 Løkken, Noline, Alfred Peter Born, Morten Duno, and John Vissing. 2015. “LAMA2-
1096 Related Myopathy: Frequency among Congenital and Limb-Girdle Muscular
1097 Dystrophies.” *Muscle & Nerve* 52 (4): 547–53. <https://doi.org/10.1002/mus.24588>.
- 1098 Lord, Megan S., Fengying Tang, Jelena Rnjak-Kovacina, James G. W. Smith, James
1099 Melrose, and John M. Whitelock. 2018. “The Multifaceted Roles of Perlecan in
1100 Fibrosis.” *Matrix Biology: Journal of the International Society for Matrix Biology* 68–
1101 69: 150–66. <https://doi.org/10.1016/j.matbio.2018.02.013>.
- 1102 McLaren, William, Laurent Gil, Sarah E. Hunt, Harpreet Singh Riat, Graham R. S. Ritchie,
1103 Anja Thormann, Paul Flicek, and Fiona Cunningham. 2016. “The Ensembl Variant
1104 Effect Predictor.” *Genome Biology* 17 (1): 122.
1105 <https://doi.org/10.1186/s13059-016-0974-4>.
- 1106 McRae, Natasha, Leonard Forgan, Bryony McNeill, Alex Addinsall, Daniel McCulloch,
1107 Chris Van der Poel, and Nicole Stupka. 2017. “Glucocorticoids Improve Myogenic
1108 Differentiation In Vitro by Suppressing the Synthesis of Versican, a Transitional
1109 Matrix Protein Overexpressed in Dystrophic Skeletal Muscles.” *International Journal*
1110 *of Molecular Sciences* 18 (12). <https://doi.org/10.3390/ijms18122629>.

- 1111 Menche, Jörg, Amitabh Sharma, Maksim Kitsak, Susan Dina Ghiassian, Marc Vidal, Joseph
1112 Loscalzo, and Albert-László Barabási. 2015. "Disease Networks. Uncovering
1113 Disease-Disease Relationships through the Incomplete Interactome." *Science (New*
1114 *York, N.Y.)* 347 (6224): 1257601. <https://doi.org/10.1126/science.1257601>.
- 1115 Mitani, Aya A., and Sebastien Haneuse. 2020. "Small Data Challenges of Studying Rare
1116 Diseases." *JAMA Network Open* 3 (3): e201965.
1117 <https://doi.org/10.1001/jamanetworkopen.2020.1965>.
- 1118 Mo, Michelle, Ha Thi Hoang, Stefan Schmidt, Robert B. Clark, and Barbara E. Ehrlich. 2013.
1119 "The Role of Chromogranin B in an Animal Model of Multiple Sclerosis." *Molecular*
1120 *and Cellular Neurosciences* 56 (September): 102–14.
1121 <https://doi.org/10.1016/j.mcn.2013.04.003>.
- 1122 Müller, Juliane S., Angela Abicht, Hans-Jürgen Christen, Rolf Stucka, Ulrike Schara,
1123 Wilhelm Mortier, Angela Huebner, and Hanns Lochmüller. 2004. "A Newly
1124 Identified Chromosomal Microdeletion of the Rapsyn Gene Causes a Congenital
1125 Myasthenic Syndrome." *Neuromuscular Disorders: NMD* 14 (11): 744–49.
1126 <https://doi.org/10.1016/j.nmd.2004.06.010>.
- 1127 Müller, Juliane S., Catherine D. Jepson, Steven H. Laval, Kate Bushby, Volker Straub, and
1128 Hanns Lochmüller. 2010. "Dok-7 Promotes Slow Muscle Integrity as Well as
1129 Neuromuscular Junction Formation in a Zebrafish Model of Congenital Myasthenic
1130 Syndromes." *Human Molecular Genetics* 19, no. 9: 1726–40.
1131 <https://doi.org/10.1093/hmg/ddq049>.
- 1132 Muona, Anu, Lauri Eklund, Timo Väisänen, and Taina Pihlajaniemi. 2002. "Developmentally
1133 Regulated Expression of Type XV Collagen Correlates with Abnormalities in
1134 Col15a1(-/-) Mice." *Matrix Biology: Journal of the International Society for Matrix*
1135 *Biology* 21 (1): 89–102.
- 1136 Nicole, Sophie, Amina Chaouch, Torberg Torbergesen, Stéphanie Bauché, Elodie de
1137 Bruyckere, Marie-Joséphine Fontenille, Morten A. Horn, et al. 2014. "Agrin
1138 Mutations Lead to a Congenital Myasthenic Syndrome with Distal Muscle Weakness
1139 and Atrophy." *Brain: A Journal of Neurology* 137 (Pt 9): 2429–43.
1140 <https://doi.org/10.1093/brain/awu160>.
- 1141 Nilsson, Anna, Maria Fälth, Xiaoqun Zhang, Kim Kultima, Karl Sköld, Per Svenningsson,
1142 and Per E. Andrén. 2009. "Striatal Alterations of Secretogranin-1, Somatostatin,
1143 Prodynorphin, and Cholecystokinin Peptides in an Experimental Mouse Model of
1144 Parkinson Disease." *Molecular & Cellular Proteomics: MCP* 8 (5): 1094–1104.
1145 <https://doi.org/10.1074/mcp.M800454-MCP200>.
- 1146 Núñez-Carpintero, Iker, Marianyela Petrizelli, Andrei Zinovyev, Davide Cirillo and Alfonso
1147 Valencia. 2021. "The multilayer community structure of medulloblastoma." *iScience*
1148 24. <https://doi.org/10.1016/j.isci.2021.102365>
- 1149 O'Connor, Emily, Ana Töpf, René P Zahedi, Sally Spendiff, Daniel Cox, Andreas Roos and
1150 Hanns Lochmüller. 2018. "Clinical and research strategies for limb-girdle congenital
1151 myasthenic syndromes." *Annals of the New York Academy of Sciences* 1412, 102–
1152 112. <https://doi.org/10.1111/nyas.13520>

- 1153 O'Connor, Emily, George Cairns, Sally Spendiff, David Burns, Stefan Hettwer, Armin
1154 Mäder, Juliane Müller, Rita Horvath, Clarke Slater, Andreas Roos, Hanns
1155 Lochmüller. 2019. "Modulation of Agrin and RhoA Pathways Ameliorates Movement
1156 Defects and Synapse Morphology in MYO9A-Depleted Zebrafish." *Cells* 8, no. 8,
1157 848. <https://doi.org/10.3390/cells8080848>.
- 1158 Ohkawara, Bisei, Macarena Cabrera-Serrano, Tomohiko Nakata, Margherita Milone,
1159 Nobuyuki Asai, Kenyu Ito, Mikako Ito, et al. 2014. "LRP4 Third β -Propeller Domain
1160 Mutations Cause Novel Congenital Myasthenia by Compromising Agrin-Mediated
1161 MuSK Signaling in a Position-Specific Manner." *Human Molecular Genetics* 23 (7):
1162 1856–68. <https://doi.org/10.1093/hmg/ddt578>.
- 1163 Ohno, K. 2003. "E-Box Mutations in the RAPSN Promoter Region in Eight Cases with
1164 Congenital Myasthenic Syndrome." *Human Molecular Genetics* 12 (7): 739–48.
1165 <https://doi.org/10.1093/hmg/ddg089>.
- 1166 Pampalakis, Georgios, Konstantinos Mitropoulos, Georgia Xeromerisiou, Efthymios
1167 Dardiotis, Georgia Deretzi, Maria Anagnostouli, Theodora Katsila, Michail Rentzos,
1168 and George P. Patrinos. 2019. "New Molecular Diagnostic Trends and Biomarkers for
1169 Amyotrophic Lateral Sclerosis." *Human Mutation* 40 (4): 361–73.
1170 <https://doi.org/10.1002/humu.23697>.
- 1171 Panchenko, M. V., W. G. Stetler-Stevenson, O. V. Trubetskoy, S. N. Gacheru, and H. M.
1172 Kagan. 1996. "Metalloproteinase Activity Secreted by Fibrogenic Cells in the
1173 Processing of Prolysyl Oxidase. Potential Role of Procollagen C-Proteinase." *The*
1174 *Journal of Biological Chemistry* 271 (12): 7113–19.
- 1175 Pearsall, Nicole, Gautam Bhattacharya, Jim Wisecarver, Joe Adams, Dominic Cosgrove, and
1176 William Kimberling. 2002. "Usherin Expression Is Highly Conserved in Mouse and
1177 Human Tissues." *Hearing Research* 174, no. 1: 55–63.
1178 [https://doi.org/10.1016/S0378-5955\(02\)00635-4](https://doi.org/10.1016/S0378-5955(02)00635-4).
- 1179 Pedrosa-Domellöf, F., I. Virtanen, and L. E. Thornell. 1995. "Tenascin Is Present in Human
1180 Muscle Spindles and Neuromuscular Junctions." *Neuroscience Letters* 198 (3): 173–
1181 76.
- 1182 Pénisson-Besnier, Isabelle, Valérie Allamand, Philippe Beurrier, Ludovic Martin, Joost
1183 Schalkwijk, Ivonne van Vlijmen-Willems, Corine Gartioux, et al. 2013. "Compound
1184 Heterozygous Mutations of the TNXB Gene Cause Primary Myopathy." *Neuromuscular*
1185 *Disorders: NMD* 23 (8): 664–69.
1186 <https://doi.org/10.1016/j.nmd.2013.04.009>.
- 1187 Petryszak, Robert, Maria Keys, Y. Amy Tang, Nuno A. Fonseca, Elisabet Barrera, Tony
1188 Burdett, Anja Füllgrabe, et al. 2016. "Expression Atlas Update—an Integrated
1189 Database of Gene and Protein Expression in Humans, Animals and Plants." *Nucleic*
1190 *Acids Research* 44 (D1): D746–52. <https://doi.org/10.1093/nar/gkv1045>.
- 1191 Petukhova, Lynn, Yutaka Shimomura, Muhammad Wajid, Prakash Gorroochurn, Susan E.
1192 Hodge, and Angela M. Christiano. 2009. "The Effect of Inbreeding on the
1193 Distribution of Compound Heterozygotes: A Lesson from Lipase H Mutations in
1194 Autosomal Recessive Woolly Hair/Hypotrichosis." *Human Heredity* 68 (2): 117–30.

- 1195 <https://doi.org/10.1159/000212504>.
- 1196 Piñero, Janet, Àlex Bravo, Núria Queralt-Rosinach, Alba Gutiérrez-Sacristán, Jordi Deu-
1197 Pons, Emilio Centeno, Javier García-García, Ferran Sanz, and Laura I. Furlong. 2017.
1198 “DisGeNET: A Comprehensive Platform Integrating Information on Human Disease-
1199 Associated Genes and Variants.” *Nucleic Acids Research* 45 (D1): D833–39.
1200 <https://doi.org/10.1093/nar/gkw943>.
- 1201 Pio-Lopez, Léo, Alberto Valdeolivas, Laurent Tichit, Élisabeth Remy, Anaïs Baudot. 2021.
1202 “MultiVERSE: a multiplex and multiplex-heterogeneous network embedding
1203 approach.” *Scientific reports* 11(1): 8794.
1204 <https://doi.org/10.1038/s41598-021-87987-1>.
- 1205 Ramanagoudr-Bhojappa, Ramanagouda, Blake Carrington, Mukundhan Ramaswami, Kevin
1206 Bishop, Gabrielle M. Robbins, MaryPat Jones, Ursula Harper, et al. 2018.
1207 “Multiplexed CRISPR/Cas9-Mediated Knockout of 19 Fanconi Anemia Pathway
1208 Genes in Zebrafish Revealed Their Roles in Growth, Sexual Development and
1209 Fertility.” *PLoS Genetics* 14 (12): e1007821.
1210 <https://doi.org/10.1371/journal.pgen.1007821>.
- 1211 Richard, P., K. Gaudon, F. Andreux, E. Yasaki, C. Prioleau, S. Bauché, A. Barois, et al.
1212 2003. “Possible Founder Effect of Rapsyn N88K Mutation and Identification of Novel
1213 Rapsyn Mutations in Congenital Myasthenic Syndromes.” *Journal of Medical
1214 Genetics* 40 (6): e81.
- 1215 Rodríguez Cruz, Pedro M., Jacqueline Palace, Hayley Ramjattan, Sandeep Jayawant,
1216 Stephanie A. Robb, and David Beeson. 2015. “Salbutamol and Ephedrine in the
1217 Treatment of Severe AChR Deficiency Syndromes.” *Neurology* 85 (12): 1043–47.
1218 <https://doi.org/10.1212/WNL.0000000000001952>.
- 1219 Rodríguez Cruz, Pedro M., Jacqueline Palace, and David Beeson. 2018. “The Neuromuscular
1220 Junction and Wide Heterogeneity of Congenital Myasthenic Syndromes.”
1221 *International Journal of Molecular Sciences* 19 (6).
1222 <https://doi.org/10.3390/ijms19061677>.
- 1223 Rogers, Robert S., and Hiroshi Nishimune. 2017. “The Role of Laminins in the Organization
1224 and Function of Neuromuscular Junctions.” *Matrix Biology: Journal of the
1225 International Society for Matrix Biology* 57–58: 86–105.
1226 <https://doi.org/10.1016/j.matbio.2016.08.008>.
- 1227 Sadeh, Menachem, Xin-Ming Shen, and Andrew G. Engel. 2011. “Beneficial Effect of
1228 Albuterol in Congenital Myasthenic Syndrome with Epsilon-Subunit Mutations.”
1229 *Muscle & Nerve* 44, no. 2: 289–91. <https://doi.org/10.1002/mus.22153>.
- 1230 Saint-Amant, Louis and Pierre Drapeau. “Time Course of the Development of Motor
1231 Behaviors in the Zebrafish Embryo.” 1998. *Journal of Neurobiology* 37, no. 4: 622–
1232 32. [https://doi.org/10.1002/\(sici\)1097-4695\(199812\)37:4<622::aid-neu10>3.0.co;2-s](https://doi.org/10.1002/(sici)1097-4695(199812)37:4<622::aid-neu10>3.0.co;2-s).
- 1233 Saito, Rintaro, Michael E Smoot, Keiichiro Ono, Johannes Ruschinski, Peng-Liang Wang,
1234 Samad Lotia, Alexander R Pico, Gary D Bader, and Trey Ideker. 2012. “A Travel
1235 Guide to Cytoscape Plugins.” *Nature Methods* 9 (11): 1069–76.
1236 <https://doi.org/10.1038/nmeth.2212>.

- 1237 Schindelin, Johannes, Ignacio Arganda-Carreras, Erwin Frise, Verena Kaynig, Mark Longair,
1238 Tobias Pietzsch, Stephan Preibisch, Curtis Rueden, Stephan Saalfeld, Benjamin
1239 Schmid, Jean-Yves Tinevez, Daniel James White, Volker Hartenstein, Kevin Eliceiri,
1240 Pavel Tomancak and Albert Cardona. 2012. “Fiji - an Open Source platform for
1241 biological image analysis.” *Nature Methods* 9, 10.1038/nmeth.2019.
1242 <https://doi.org/10.1038/nmeth.2019>
- 1243 Schwaller, Fred, Valérie Bégay, Gema García-García, Francisco J. Taberner, Rabih
1244 Moshourab, Brennan McDonald, Trevor Docter, Johannes Kühnemund, Julia Ojeda-
1245 Alonso, Ricardo Paricio-Montesinos, Stefan G. Lechner, James F. A. Poulet, Jose M.
1246 Millan and Gary R. Lewin. 2021. “USH2A is a Meissner’s Corpuscle Protein
1247 Necessary for Normal Vibration Sensing in Mice and Humans.” *Nature Neuroscience*
1248 24, no. 1: 74–81. <https://doi.org/10.1038/s41593-020-00751-y>.
- 1249 Senderek, Jan, Juliane S Müller, Marina Dusl, Tim M. Strom, Velina Guergueltcheva,
1250 Irmgard Diepolder, Steven H. Laval, Susan Maxwell, Judy Cossins, Sabine Krause,
1251 Nuria Muelas, Juan J. Vilchez, Jaume Colomer, Cecilia Jimenez Mallebrera, Andres
1252 Nascimento, Shahriar Nafissi, Ariana Kariminejad, Yalda Nilipour, Bitra Bozorgmehr,
1253 Hossein Najmabadi, Carmelo Rodolico, Jörn P Sieb, Ortrud K. Steinlein, Beate
1254 Schlotter, Benedikt Schoser, Janbernd Kirschner, Ralf Herrmann, Thomas Voit,
1255 Anders Oldfors, Christopher Lindbergh, Andoni Urtizberea, Maja von der Hagen,
1256 Angela Hübner, Jacqueline Palace, Kate Bushby, Volker Straub, David Beeson,
1257 Angela Abicht and Hanns Lochmüller 2011. “Hexosamine Biosynthetic Pathway
1258 Mutations Cause Neuromuscular Transmission Defect.” *American Journal of Human
1259 Genetics* 88, no. 2: 162–72. <https://doi.org/10.1016/j.ajhg.2011.01.008>.
- 1260 Sorensen, Jacob R., Caitlin Skousen, Alex Holland, Kyle Williams, and Robert D. Hyldahl.
1261 2018. “Acute Extracellular Matrix, Inflammatory and MAPK Response to
1262 Lengthening Contractions in Elderly Human Skeletal Muscle.” *Experimental
1263 Gerontology* 106: 28–38. <https://doi.org/10.1016/j.exger.2018.02.013>.
- 1264 Stum, Morgane, Claire-Sophie Davoine, Savine Vicart, Léna Guillot-Noël, Haluk Topaloglu,
1265 Francisco Javier Carod-Artal, Hülya Kayserili, et al. 2006. “Spectrum of HSPG2
1266 (Perlecan) Mutations in Patients with Schwartz-Jampel Syndrome.” *Human Mutation*
1267 27 (11): 1082–91. <https://doi.org/10.1002/humu.20388>.
- 1268 Swuec, Paolo, Ludovic Renault, Aaron Borg, Fenil Shah, Vincent J. Murphy, Sylvie van
1269 Twest, Ambrosius P. Snijders, Andrew J. Deans, and Alessandro Costa. 2017. “The
1270 FA Core Complex Contains a Homo-Dimeric Catalytic Module for the Symmetric
1271 Mono-Ubiquitination of FANCI-FANCD2.” *Cell Reports* 18 (3): 611–23.
1272 <https://doi.org/10.1016/j.celrep.2016.11.013>.
- 1273 Sztal, Tamar E., Avnika A. Ruparelia, Caitlin Williams, and Robert J. Bryson-Richardson.
1274 2016. “Using Touch-Evoked Response and Locomotion Assays to Assess Muscle
1275 Performance and Function in Zebrafish.” *Journal of Visualized Experiments : JoVE*,
1276 no. 116: 54431. <https://doi.org/10.3791/54431>.
- 1277 Thompson, Rachel, Anastasios Papakonstantinou Ntalas, Sergi Beltran, Ana Töpf, Eduardo
1278 de Paula Estephan, Kiran Polavarapu, Peter A. C. ’t Hoen, Paolo Missier, and Hanns

- 1279 Lochmüller. 2019. “Increasing Phenotypic Annotation Improves the Diagnostic Rate
1280 of Exome Sequencing in a Rare Neuromuscular Disorder” *Human Mutation*, June.
1281 <https://doi.org/10.1002/humu.23792>.
- 1282 Tinevez, Jean-Yves, Nick Perry, Johannes Schindelin, Genevieve M. Hoopes, Gregory D.
1283 Reynolds, Emmanuel Laplantine, Sebastian Y. Bednarek, Spencer L. Shorte, and
1284 Kevin W. Eliceiri. “TrackMate: An Open and Extensible Platform for Single-Particle
1285 Tracking.” *Methods (San Diego, Calif.)* 115 (February 15, 2017): 80–90.
1286 <https://doi.org/10.1016/j.ymeth.2016.09.016>.
- 1287 Valdeolivas, Alberto, Laurent Tichit, Claire Navarro, Sophie Perrin, Gaëlle Odelin, Nicolas
1288 Levy, Pierre Cau, Elisabeth Remy, and Anaïs Baudot. 2019. “Random Walk with
1289 Restart on Multiplex and Heterogeneous Biological Networks.” *Bioinformatics*
1290 *(Oxford, England)* 35 (3): 497–505. <https://doi.org/10.1093/bioinformatics/bty637>.
- 1291 Vanhaesebrouck, An E, Richard Webster, Susan Maxwell, Pedro M Rodriguez Cruz, Judith
1292 Cossins, James Wickens, Wei-wei Liu, et al. 2019. “B2-Adrenergic Receptor
1293 Agonists Ameliorate the Adverse Effect of Long-Term Pyridostigmine on
1294 Neuromuscular Junction Structure.” *Brain* 142, no. 12: 3713–27.
1295 <https://doi.org/10.1093/brain/awz322>.
- 1296 Vázquez, Miguel, Rubén Nogales, Pedro Carmona, Alberto Pascual, and Juan Pavón. 2010.
1297 “Rbbt: A Framework for Fast Bioinformatics Development with Ruby.” In *Advances*
1298 *in Bioinformatics*, edited by Miguel P. Rocha, Florentino Fernández Riverola, Hagit
1299 Shatkey, and Juan Manuel Corchado, 74:201–8. Berlin, Heidelberg: Springer Berlin
1300 Heidelberg. https://doi.org/10.1007/978-3-642-13214-8_26.
- 1301 Voermans, N. C., and B. G. van Engelen. 2008. “Differential Diagnosis of Muscular
1302 Hypotonia in Infants: The Kyphoscoliotic Type of Ehlers-Danlos Syndrome (EDS
1303 VI).” *Neuromuscular Disorders: NMD* 18 (11): 906; author reply 907.
1304 <https://doi.org/10.1016/j.nmd.2008.05.016>.
- 1305 Voermans, Nicol C., Karin Gerrits, Baziel G. van Engelen, and Arnold de Haan. 2014.
1306 “Compound Heterozygous Mutations of the TNXB Gene Cause Primary Myopathy.”
1307 *Neuromuscular Disorders: NMD* 24 (1): 88–89.
1308 <https://doi.org/10.1016/j.nmd.2013.10.007>.
- 1309 Wang, Dan-Ni, Zhi-Qiang Wang, Yu-Qing Chen, Guo-Rong Xu, Min-Ting Lin, and Ning
1310 Wang. 2018. “Limb-Girdle Muscular Dystrophy Type 2I: Two Chinese Families and
1311 a Review in Asian Patients.” *The International Journal of Neuroscience* 128 (3): 199–
1312 207. <https://doi.org/10.1080/00207454.2017.1380640>.
- 1313 Wen, Hua, Michael W. Linhoff, Matthew J. McGinley, Geng-Lin Li, Glen M. Corson, Gail
1314 Mandel, and Paul Brehm. 2010. “Distinct Roles for Two Synaptotagmin Isoforms in
1315 Synchronous and Asynchronous Transmitter Release at Zebrafish Neuromuscular
1316 Junction.” *Proceedings of the National Academy of Sciences of the United States of*
1317 *America* 107, no. 31: 13906–11. <https://doi.org/10.1073/pnas.1008598107>.
- 1318 Whicher, Danielle, Sarah Philbin, and Naomi Aronson. 2018. “An Overview of the Impact of
1319 Rare Disease Characteristics on Research Methodology.” *Orphanet Journal of Rare*
1320 *Diseases* 13 (1): 14. <https://doi.org/10.1186/s13023-017-0755-5>.

- 1321 Xu, Zhuo, Naoki Ichikawa, Keisuke Kosaki, Yoshihiko Yamada, Takako Sasaki, Lynn Y.
1322 Sakai, Hisashi Kurosawa, Nobutaka Hattori, and Eri Arikawa-Hirasawa. 2010.
1323 “Perlecan Deficiency Causes Muscle Hypertrophy, a Decrease in Myostatin
1324 Expression, and Changes in Muscle Fiber Composition.” *Matrix Biology: Journal of*
1325 *the International Society for Matrix Biology* 29 (6): 461–70.
1326 <https://doi.org/10.1016/j.matbio.2010.06.001>.
- 1327 Yang, Kunfang, Hongyi Cheng, Fang Yuan, Linyi Meng, Rongrong Yin, Yuanfeng Zhang,
1328 Simei Wang, et al. 2018. “CHRNE Compound Heterozygous Mutations in Congenital
1329 Myasthenic Syndrome: A Case Report.” *Medicine* 97 (17): e0347.
1330 <https://doi.org/10.1097/MD.00000000000010347>.
- 1331 Zhong, Jingzi, Gang Chen, Yiwu Dang, Haixia Liao, Jiapeng Zhang, and Dan Lan. 2017.
1332 “Novel Compound Heterozygous PLEC Mutations Lead to Early-onset Limb-girdle
1333 Muscular Dystrophy 2Q.” *Molecular Medicine Reports* 15 (5): 2760–64.
1334 <https://doi.org/10.3892/mmr.2017.6309>.
- 1335 Zitnik, Marinka, and Jure Leskovec. 2017. “Predicting Multicellular Function through Multi-
1336 Layer Tissue Networks.” *Bioinformatics (Oxford, England)* 33 (14): i190–98.
1337 <https://doi.org/10.1093/bioinformatics/btx252>.